AD–A230 531

(1)

DTIC
ELECTE
JAN 07 1991
D
D

DEPARTMENT OF THE AIR FORCE

AIR UNIVERSITY

AIR FORCE INSTITUTE OF TECHNOLOGY

Wright-Patterson Air Force Base, Ohio

91 1 3 158

AFIT/GE/ENG/90D-61

DTIC
ELECTE
JAN 07 1991
S D
D

ESTABLISHMENT OF A FABRICATION AND
MEASUREMENT CAPABILITY FOR APERTURE-FED
STACKED PATCH MICROSTRIP ANTENNAS AT THE
AIR FORCE INSTITUTE OF TECHNOLOGY

THESIS

Christopher I. Terry
Captain, USAF

AFIT/GE/ENG/90D-61

AFIT/GE/ENG/90D-61

ESTABLISHMENT OF A FABRICATION AND MEASUREMENT CAPABILITY

FOR APERTURE-FED STACKED PATCH MICROSTRIP ANTENNAS

AT THE AIR FORCE INSTITUTE OF TECHNOLOGY

THESIS

Presented to the Faculty of the School of Engineering

of the Air Force Institute of Technology

Air University

In Partial Fulfillment of the

Requirements for the Degree of

Master of Science in Electrical Engineering

Christopher I. Terry, B.S.E.E.

Captain, USAF

December 1990

Preface

The purpose of this study was to develop a simple
fabrication and measurement capability for aperture-fed
stacked patch microstrip antennas. This capability will
greatly enhance the ability of the Air Force Institute of
Technology (AFIT) to actively research broader bandwidth
microstrip patch antennas. The final measurements performed
on the two antennas fabricated were provided to Captain Ron
Erwert and Captain William Irvin for comparison with pattern
predictions generated through their thesis efforts to model
this antenna with Green's functions.

While this study details the efforts required to
fabricate and measure two microstrip antennas, it is
intended to provide insight to any individual or
organization interested in starting an active investigation
into microstrip patch antennas in general. It is important
to note that this study avoided the use of outside
organizations in an attempt to create a completely self-
contained fabrication and measurement capability within
AFIT.

This study produced two microstrip antennas described
in the PhD dissertation of Dr. Nirod K. Das. While the
antennas performed less than optimally, the value of this
study is not diminished. These efforts lay a sound

Table of Contents

List of Figures

AFIT/GE/ENG/90D-61

Abstract

Much time and effort has been applied to accurately model aperture-fed stacked patch microstrip antennas at the Air Force Institute of Technology (AFIT). The results of this study provide AFIT the capability to fabricate and measure these antennas for comparison of measured radiation characteristics to the predicted characteristics. Basic microstrip patch antenna theory is reviewed, as well as the motivation leading to the development of aperture-fed stacked patch microstrip antennas. The fabrication process used to produce the two antennas manufactured for this study is described in detail. The construction of a small anechoic chamber for pattern measurements is discussed, and measurements of the return loss, VSWR, input impedance, and principal plane radiation patterns for the two antennas of this study are provided. Although the two fabricated antennas did not operate optimally due to under cutting during the etching process, the measurement results show the broader bandwidth characteristic of the stacked patch design. The results of this study are most useful as a guide to researchers starting an active microstrip patch antenna investigation.

ESTABLISHMENT OF A FABRICATION AND MEASUREMENT CAPABILITY FOR APERTURE-FED STACKED PATCH MICROSTRIP ANTENNAS AT THE AIR FORCE INSTITUTE OF TECHNOLOGY

I. Introduction

Background

Microstrip antennas are of great interest to the aerospace community because of their many inherent advantages over other antenna designs. Because of these advantages, the microstrip antenna is becoming increasingly important to the U. S. Air Force and the Air Force Institute of Technology (AFIT).

Basic Microstrip Antenna Advantages. The basic microstrip antenna's lightweight and small volume make it an ideal candidate for use on satellites and missiles. This antenna is also relatively easy to fabricate. Because of the low profile and capability to conform the microstrip antenna to complex body shapes, it can be designed into nearly any airframe. It is also possible to integrate a feed network onto the same substrate as the antenna, further reducing the space required for the aircraft's antenna

system. This integrated feed network advantage is especially important when the microstrip antenna is used in its primary role as an element in an array.

Basic Microstrip Antenna Disadvantages. The basic microstrip antenna has four primary disadvantages. These disadvantages are its very narrow bandwidth (approximately 2 percent), poor isolation between the feedline and the radiating patch, contradictive optimum relative permittivities of the feed network and radiating patch, and competition for substrate area between the feed network and the radiating patch. In particular, an antenna with a two percent bandwidth has a very limited usefulness. Poor feedline isolation results in unwanted radiation from the feed network, corrupting the radiation pattern of the antenna. A high permittivity substrate is best for feedlines, while a low permittivity substrate is best for the radiating patch. Thus, a compromise in permittivities is often necessary. Optimal use of the available substrate surface area is vital, particularly when this antenna is used as an element in an array. For this reason, any substrate surface area used for the feed network is area that cannot be used for the radiating patches of an antenna array. For many aerospace applications, these disadvantages must be overcome if the microstrip antenna is going to be useful.

Problem Statement

Much time and effort has been spent recently in the scientific community and at AFIT to accurately model the aperture-fed stacked patch microstrip antenna. In contrast to the advances in accurate modeling, there is currently a lack of an established fabrication and measurement capability for microstrip antennas at AFIT. The purpose of this thesis is to establish the capability at AFIT to implement a design through fabrication and measure aperture-fed stacked patch microstrip antennas for verification of the theoretical models.

Research Objectives

This research seeks to lay the foundation for future work with microstrip antennas at AFIT. First, through a thorough literature review, designs for simple stacked patch aperture-fed microstrip antennas will be selected. Secondly, these designs will be used to fabricate the microstrip antennas for measurement. Lastly, these antennas will be tested to determine their radiation patterns, input impedances, and VSWR bandwidths. Each of these three steps will be carefully documented to provide researchers a guide for use during future investigations of microstrip antennas.

Approach

Aperture-fed stacked patch antennas have been designed and used for numerous applications. The progress during the development of this antenna is well documented in the literature. This research project relies heavily on this documentation.

Design. The literature reveals that the patch sizes of the aperture-fed stacked patch microstrip antenna should be near one-half wavelength referred to the resonant frequency. To maximize design tolerances, an antenna with a center frequency near 3.8 GHz will be used. The substrates will be selected based on those specified in the chosen design. All other physical dimensions will also be determined from the design documented in the literature.

Fabrication. Once the entire design is determined, accurate drawings will be created. These drawings will be used to produce the proper masks to be used for the photo etching process. Once the photo etching is completed, the antenna's dimensions and electrical characteristics will be checked to ensure they are within acceptable tolerance levels.

Testing. The finished antenna will be tested in an antenna measurement chamber at AFIT. This chamber will be built as part of this project. A network analyzer will be used to determine the antenna's actual center frequency, E

4

and H plane radiation patterns, input impedance, and VSWR bandwidth. The antenna will be used as the receiving antenna with a standard gain horn antenna used as the transmitting antenna.

Materials and Equipment

This research project will use substrate material obtained from the manufacturer and photo etching equipment and materials in place in the Cooperative Electronics Materials and Processes Laboratory at Wright-Patterson Air Force Base. A new antenna measurement chamber will be built to make all radiation characteristic measurements. This measurement chamber will be equipped with an HP8349B frequency synthesizer and HP8510B network analyzer. The HP8510B network analyzer will be used in the manual mode during each of the measurements.

Summary of Remaining Chapters

Chapter II is a review of the historical development of microstrip antennas and present design capabilities for these antennas. Particular attention is paid to the theory of operation of the basic microstrip antenna, as well as the motivation behind the development of the aperture-fed stacked patch microstrip antenna. Fabrication and

measurement concerns addressed in the literature are also discussed.

Chapter III describes the selected antenna designs and the fabrication of those designs. General, as well as specific, techniques for masking and etching processes are discussed. The equipment used and the support provided for this thesis project are described in detail.

Chapter IV describes the measurement facility and techniques used during this study. Also, the results of the measurements conducted are included here. In particular, VSWR, return loss, input impedance and radiation pattern plots are provided.

Chapter V contains the conclusions reached from this study and recommendations for further research in this area.

II. Historical Development and Current Efforts

Background

Microstrip antennas are not a new concept. The development of microstrip transmission lines, the foundation for all microstrip devices, was first reported by Greig and Englemann in 1952 (13:12). Soon after, in 1953, Deschamps proposed the microstrip radiator and the first published reference to a microstrip antenna array quickly followed in 1955 in a patent application by Gutton and Bassinot (13:13). Due to the lack of sufficient fabrication technology, practical microstrip antennas were not fabricated until nearly twenty years later. The 1970's saw greatly improved theoretical models and photo etch techniques which made the microstrip antenna feasible. The first practical antennas were developed in the early 1970's by Howell and Munson, enabling extensive research and development of microstrip antennas and arrays (2:1).

Basic Microstrip Patch Antennas (2:2-10,317-324)

In its simplest form, Bahl and Bhartia have defined a microstrip antenna as "a radiating patch on one side of a dielectric substrate ($\epsilon_r \leq 10$),which has a ground plane on the other side" (2:2). Bhattacharjee and others have

successfully modeled the center-fed rectangular microstrip antenna of length $\lambda/2$ as simply a lossy half-wavelength open-circuited transmission line (4:1169). The selection of the substrate's dielectric constant is a matter of trade-offs. A low dielectric constant will enhance the fringing fields which account for the radiation. On the other hand, a particular application may require a substrate that is heat resistant and a low dielectric substrate material may not be available that satisfies this condition. Also, the antenna may be for low frequency operation which requires the use of high dielectric substrates to keep the size small.

Radiation Mechanism. (2:4-16) Bahl and Bhartia describe the radiation from a rectangular microstrip patch antenna. An example of this type of microstrip antenna is shown in Figure 1(a). The patch length is designed to be $\lambda/2$ long, where λ is the wavelength corresponding to the resonant frequency. If the electric fields along the width and thickness of the microstrip structure are modeled as constant, the electric field of the radiator is shown in Figure 1(b), with the fields varying along the length of the patch. The dominant radiation mechanisms are the fringing fields at the open-circuited edges of the patch. Since the fields can be resolved into components normal and tangential to the ground plane, it is important to note that the normal

8
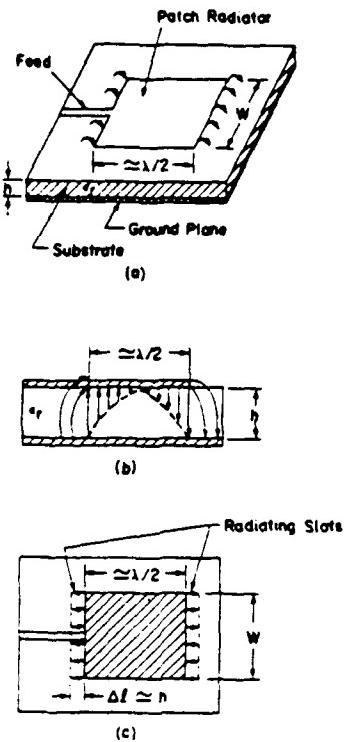
Figure 1. (a) Rectangular Patch Antenna, (b) Side View, (c) Top View (2:6)

components are out of phase because the patch length is $\lambda/2$ long. This will result in the far-field produced by the normal components canceling at broadside. Conversely, the tangential components are in phase and add to a maximum at broadside. Thus, the far-field pattern at broadside of this antenna is determined by the tangential components alone. This feature allows the structure to be represented by two in-phase radiating slots $\lambda/2$ apart as shown in Figure 1(c).

Patch Resonator. "A rectangular patch resonator consists of a microstrip line q half-wavelengths long (q=1,2,3...)" (13:60). This mechanism is similar to exciting field modes in a waveguide, and for antenna applications the best choice is q=1, since higher order modes tend to distort the radiation patterns and impedance. Thus, it is the electrical length of the resonating patch that is critical in determining the resonant frequency of the antenna (13:60-61). To complicate matters, the electrical length of the patch is dependent on the propagation velocity within the patch. This velocity varies with relative permittivity, patch width, and operating frequency (19:9). The width of the patch radiator is also important in determining the antenna's efficiency and which order of modes will be supported by the patch (1:122). Although this paper will not specifically address alternate patch geometries, it is interesting to note that many different shapes, such as circular and triangular, have been successfully used in microstrip patch antenna applications (7:251).

Feed Mechanisms. (13:69-71) Many different techniques for the excitation of the patch radiator exist. The most widely used method is to etch a microstrip transmission line on the same substrate as the radiator, as shown in Figure 2(a). The advantage of this technique is ease of
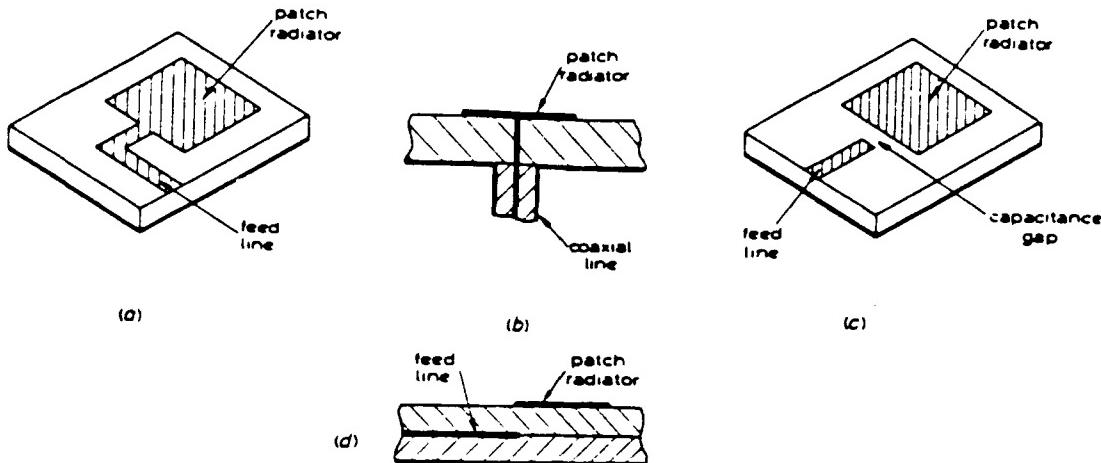
Figure 2. Feed Methods for Microstrip Patch Antennas
(13:70)

fabrication, but a serious disadvantage arises due to the

high-radiation impedance at the patch edge. This impedance

problem creates the requirement for a matching network.

Also, unwanted radiation from the microstrip feedline

occurs, corrupting the desired radiation pattern of the

antenna. To avoid the impedance problem, the feed voltage

can be directly applied to a point on the patch away from

the high-impedance edges. This design is shown in

Figure 2(b) where a coaxial line is used with the inner

element connected to the patch radiator and the outer

element connected to the ground plane. Capacitive coupling

may also be used to excite the radiator, as shown in Figure

2(c). This method is difficult to design and produce

accurately. As a variation of the capacitive coupling

technique, a multilayer dielectric with the feedlines closer

11

to the ground plane than the radiator may be used. An example of this method is shown in Figure 2(d). The feedline and the radiator may be directly coupled with a pin or coupled by the fringing fields of the feedline. Both direct coupling and fringing field coupling minimize unwanted feedline radiation and leave more space available for patch radiators on the antenna's outer surface.

Aperture-Fed Stacked Patch Microstrip Antennas

As mentioned in Chapter 1, one of the primary disadvantages of the basic microstrip patch antenna is its inherent narrow bandwidth. Bahl and Bhartia report a bandwidth of about two percent as typical for a standard microstrip antenna (1:122-126). As demonstrated by Tsao and others, this disadvantage can be eliminated through the use of multiple stacked radiating patches (24:936-939).

Stacked Patches. Figure 3 shows a microstrip antenna design implementing stacked radiating patches. The reason for using the stacked patch configuration is to increase the bandwidth of the antenna (15:624; 6:767). Fundamentally, the bandwidth of microstrip radiators is directly proportional to the distance between the ground plane and the radiating element because an increase in separation distance correlates to an increase in the characteristic impedance (3:495). Although this reasoning would suggest
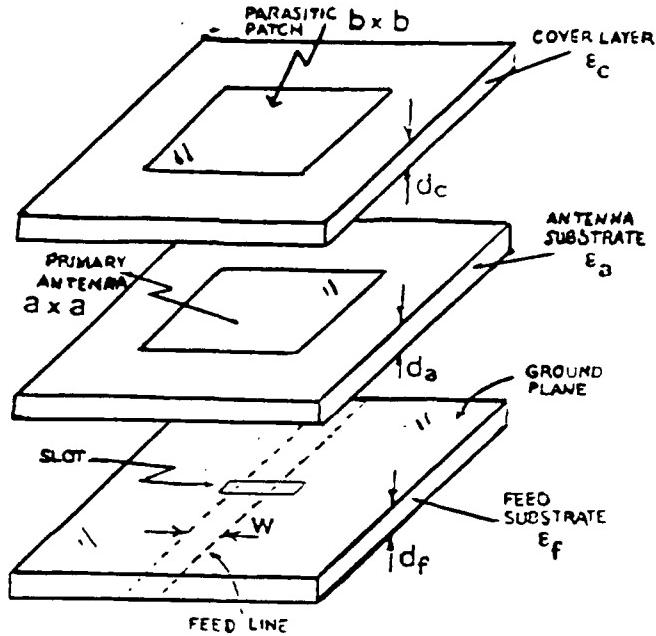
Figure 3. Aperture-Fed Stacked Patch Microstrip Antenna
           (8:2)

the use of thicker substrates to increase bandwidth, thicker

substrates introduce the excitation of surface waves and

higher order modes with z-dependence (with z the thickness

axis) resulting in pattern distortion and lower efficiency.

By stacking the patches and capacitively coupling them, the

antenna's characteristic impedance is changed by

significantly increasing the effective separation distance

over the basic microstrip antenna configuration (13:13-14).

Figure 3 shows a simple two-layer stacked patch antenna with

the lower patch (radiating patch) and the upper patch

(parasitic patch) of equal dimensions. This is not always

13

the case, as antennas have been designed with more than two
patches stacked (15:624-625), as well as incorporating
stacked patches of unequal dimensions (2:74). The unequally
dimensioned stacked-patch structures can be designed to
allow use of the antenna over two resonant frequencies. The
smaller patch is placed on top of the larger patch, which
operates as the ground plane when the smaller patch is
resonating (2:75). The smaller patch is transparent to the
larger patch when the larger patch is resonating. Figure 4
shows an example of this configuration. While the primary
reason for the stacked-patch design is to improve the
bandwidth of the basic patch antenna, R.Q. Lee and others
have shown that the stacked-patch design results in three
separate regions of operation depending on separation
distance between the patches. The primary region for the
smallest spacing yields moderate gain and improved
bandwidth. As the spacing increases, a region of very
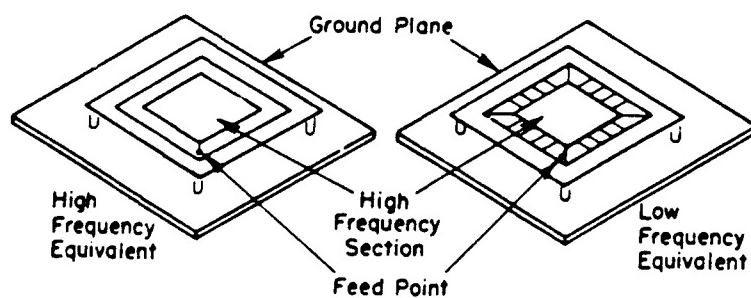
Figure 4. Dual Frequency Microstrip Patch Antenna (2:74)

narrow bandwidth occurs. The third region is defined for the largest spacing and results in narrow bandwidth but high gain (16:1070-1072).

Feed Mechanism. D.M. Pozar first proposed using aperture coupling to feed a microstrip antenna (21:49). Using electromagnetic coupling through an aperture in the ground plane located above the microstrip feedline and directly below the radiating patch has many advantages over alternate methods of exciting the patch resonator. Schaubert and Pozar describe two critical advantages of the aperture feed, while Das and Pozar describe a third. First, this method enables designers to use low dielectric substrate material for the antenna, while using higher dielectric material for the active circuits. Second, this method frees up space on the top substrate for patch radiator use since no space on this substrate is required for microstrip feedlines (23:135-137). Third, since the feedline and the radiating patch are on opposite sides of the intervening ground plane, the desired isolation between these components is easily maintained (8:1). Although via connection probes can be used to maximize the available surface space, "these via connections are increasingly difficult to fabricate as the frequency increases" (23:136). This third advantage is not trivial since this antenna is commonly used in arrays consisting of hundreds or thousands

of elements (24:936). The aperture feed works by coupling
power from the microstrip feedline through the aperture in
the ground plane to the patch resonator. This aperture must
be small in comparison to a wavelength (electrically small),
but its shape can vary. For example, Himdi and others
performed an analysis of aperture coupling in a microstrip
antenna with a rectangular aperture (11:391). This aperture
size requirement ensures that the aperture is smaller than
the resonant size of the patch and the aperture itself does
not resonate so that the bandwidth of the antenna will
remain a function of the patch (20:1137; 17:96-116). Also,
the ground plane's size should be on the order of four
wavelengths to minimize radiation pattern corruption from
surface waves induced on the ground plane (23:135-137). The
microstrip feedline below the aperture is terminated in an
open circuit a distance beyond the aperture such that the
feedline current in the vicinity of the aperture is near a
maximum for maximum coupling to the magnetic aperture
current. Thus, aperture size and length of the microstrip
feedline are variables for tuning the antenna for impedance
matching (21:50). It must be kept in mind that to determine
the proper location for the aperture in relation to the open
circuited end of the feedline, the wavelength in the
feedline must be determined. Because the fields from the
feedline extend over inhomogeneous regions (air and

dielectric), the waves cannot be purely transverse electromagnetic. The dominant mode of the transmission line will be quasi-TEM and exhibit dispersion (9:145). Therefore, it is necessary to determine the effective permittivity of the feedline. The following equations from the paper by Garidol will approximate the wavelength in the feedline (9:146-147).

$$\lambda_g = \lambda_0/\sqrt{\varepsilon_e}$$

$$\varepsilon_e \cong (\varepsilon_r + 1)/2 + \frac{[(\varepsilon_r - 1)/2]}{[1 + 10h/w]^{ab}}$$

with

$$a = 1 + 1/49\ln(\frac{(w/h)^4 + w/(52h)^2}{(w/h)^4 + 0.432})$$

$$+ 1/18.7\ln(1 + (\frac{w}{18.1h})^3)$$

$$b = [\frac{(\varepsilon_r - 0.9)}{(\varepsilon_r + 3)}]^{0.053}$$

where

ε_e = effective permittivity

ε_r = relative permittivity of substrate

h = substrate thickness

w = feedline width

λ_g = feedline wavelength

λ_0 = free space wavelength

17

These equations produce approximations accurate within 0.2%
for $0.01 \leq w/h \leq 100$ and $1 \leq \varepsilon_r \leq 128$ for striplines on
substrates backed by a solid ground plane (9:146). Once the
wavelength in the feedline is known, the aperture center is
placed one quarter wavelength from the open circuited end,
less a small distance (Δl) to account for the fringing
fields at the end of the stripline. The fringing fields at
the end of the stripline cause the line to be electrically
longer than the line's physical length. Hammerstadt
provides an equation to estimate this difference (Δl)
between electrical and physical lengths (10:268-272).

$$\Delta l = 0.412h * \frac{[\varepsilon_e + 0.3][w/h + 0.262]}{[\varepsilon_e - 0.258][w/h + 0.813]} \qquad (5)$$

where

> h = substrate thickness
>
> w = feedline width
>
> ε_e = effective permittivity from Eq (1)

Thus, the first current maximum from the open circuited end
of the line occurs at $(0.25\lambda_g - \Delta l)$. This position will
provide maximum coupling to the primary patch from the
feedline through the aperture. As a variation of this
method, the feed substrate can be oriented perpendicularly
to the antenna substrate and electromagnetically couple the

18

feedline to the patch (5:125). It is also possible to use two feedlines in phase quadrature and with an angular separation of 90 degrees to achieve circular polarization (22:64).

Fabrication Concerns

Because of the relatively narrow bandwidth of microstrip antennas, deviations in the effective electrical dimensions, variations in the permittivity of the substrate, or variations in the thickness of the substrate will cause the actual resonant frequency of the antenna to differ from the designed frequency (1:122). Tolerances of a few percent in higher dielectric constant substrates are common, while variation in substrate thickness of 5% is not uncommon. Etching accuracy is a function of the process, as well as the materials used (2:123). Fast etching agents act quickly and suffer less from under cutting the edges of the patterns. Photo etching, using light sensitive masking agents, is the primary method of fabrication for microstrip antennas. Bahl and Bhartia state that the uncertainty in manufacturing tolerances and etching accuracy introduce fabrication errors (1:122). These fabrication errors can not be avoided in a simple fabrication method, but the errors should be considered. In particular, it must be recognized that these errors will cause the antenna's

operating center frequency to be slightly different than the design center frequency. Bahl and Bhartia also state that for frequencies above 2.5 GHz and using low relative permittivity substrates, the resonant frequency is essentially independent of fluctuations in the substrate thickness and the substrate's relative permittivity. The major factor effecting the resonant frequency is the fabrication tolerance in the patch length (1:124). For high permittivity substrates, the relative permittivity is the critical parameter (1:124).

<u>Summary</u>

The microstrip patch antenna is extremely versatile. The patch geometry may be varied according to the requirements of the application, and the patch may be fed by a wide variety of methods (13:69-71). The aperture-fed stacked patch microstrip antenna offers many performance improvements over the basic patch antenna. The aperture feed provides good isolation between the feedline and the radiating patch (8:1), while providing for more efficient use of the outer substrate area. Most importantly, the stacked patch configuration overcomes the severe limitation of the basic microstrip patch antenna's narrow bandwidth (15:624).

III. Design Selection and Fabrication Methods

This chapter explains the choice of antenna design and provides all the required dimensions for fabrication. General fabrication techniques are discussed, as well as the specific techniques used to fabricate the antenna. All original artwork was created with the program MASK, which is included in Appendix A. All fabrication processes were completed at the Cooperative Electronics Materials and Processes Laboratory at Wright-Patterson Air Force Base.

Design Selection

Designing an aperture-fed stacked patch microstrip antenna is extremely difficult and time consuming. Two concurrent AFIT theses are working with Green's functions and the Method of Moments to develop a computer model to assist in the design of these antennas. Since determining an original design was well beyond the scope of this thesis, two previously implemented designs were used. Since these designs were the first microstrip antennas fabricated at AFIT, relatively simple designs were needed. Dr. Nirod K. Das describes in detail in his PhD dissertation the antenna designs that were used for this work (8:160-168). Figure 5 shows the antenna design selected. This antenna has two

PARASITIC PATCH
(a × a mm)

PRIMARY PATCH
(25.0 mm × 25.0 mm)

GROUND PLANE
APERTURE
(15 mm × 11 mm)

FEEDLINE: 5 mm × 35.22 mm

ALL LAYERS 1.58 mm THICK ; RELATIVE PERMITTIVITY = 2.2

PRIMARY ANTENNA: a=25 mm   SECONDARY ANTENNA: a=26.5 mm
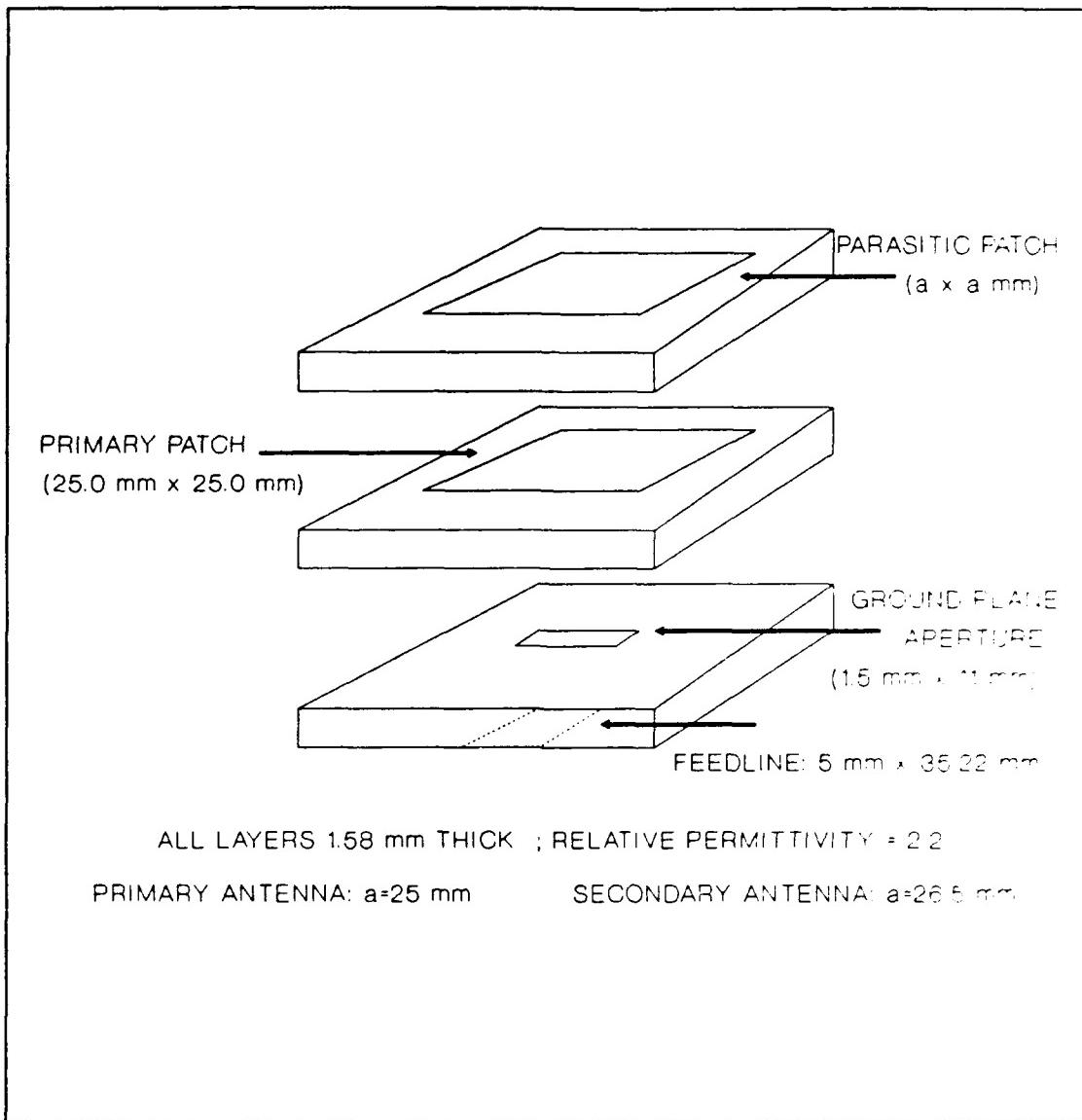
Figure 5.   Selected Antenna Design

primary advantages which ease the fabrication process.
First, the antenna is designed with a center frequency
region near 3.65 GHz. This relatively low frequency allows
for larger design tolerances in the fabrication process,
since all tolerances are in terms of wavelength. Second,
Das's design uses the same substrate material for all three

22

layers. While this does not optimally use the aperture-feed

configuration, it does make for a simpler design. Using

identical substrate material for all the layers avoids

"matching" problems between the layers separated by the

ground plane containing the aperture. For example, if

substrates of differing relative permittivities are used on

opposite sides of the aperture, the electrical size of the

aperture will appear to differ according to which side it is

viewed from. This design complexity is avoided when

substrates with identical permittivities are used. As can

be seen in Figure 5, Das's basic design uses identical

patches for the primary antenna and the parasitic element.

A second design was implemented with all but the dimensions

of the parasitic patch held constant. The second antenna

used a square parasitic patch 2.65 cm by 2.65 cm, as opposed

to the 2.5 cm by 2.5 cm square parasitic patch of the basic

design. By fabricating both antennas, it was possible to

observe the changes in the radiation characteristics of the

basic antenna when only the parasitic patch is altered. Dr.

Das provided all the required dimensions in his

dissertation, except for the distance from the open

circuited end of the microstrip feedline to the point

directly under the center of the aperture. Since it is

desired to have the aperture directly above a current

maximum, the aperture must be placed one quarter of a

resonant wavelength from the open-circuited end of the feedline less a small distance which accounts for the fringing field at the end of the stripline. This distance was computed using the effective permittivity equation and the wavelength equation (Eqs (1) through (4)) as discussed in Chapter 2. All the dimensions are included in Figure 5. For practical reasons, four alignment holes in the substrate were added to assist in joining the layers during measurement. Four nylon screws were used in the holes. Also, because of the width of the feedline, it was necessary to miter the feedline at the connector-feedline junction to avoid shorting out the connector. A 15 degree miter is best to avoid drastically changing the characteristics of the feedline (18).

Antenna Fabrication

Once the antenna design is determined, the proper dielectric substrate material must be acquired from a manufacturer. The photo masks must be produced for use during the photo-etch process. Once the masks are finished and the substrate material is in hand, the antenna can be fabricated.

Substrate Material. In order to implement the selected design, dielectric material with a relative permittivity of 2.2 was required. Also, the antenna and parasitic patch

layers required copper cladding on only one side, while the feed substrate required copper cladding on both sides. After researching available technical catalogs, it was determined that only Rogers Corporation of Chandler, Arizona had the required substrate material readily available. Through a cooperative program administered by the Rogers Corporation for participating educational institutions, Rogers donated all the required substrate material for this project. Two 12" by 18" Duroid 5880 dielectric sheets were provided. Each sheet was cladded with 1/2 ounce of copper per square foot on both sides and the sheet was 1/16" thick with a relative permittivity of 2.2 . Each sheet arrived covered with a clear adhesive-coated plastic to protect the Duroid sheet against oxidation. This protective sheet was left in place until the start of the fabrication process. Upon receipt, one sheet was cut into rough 2" by 2" squares with a hacksaw to ease handling during the fabrication process.

Mask Creation. A crucial step in the fabrication process is the creation of accurate drawings of the antenna structures. The best technique for a particular application is dependent upon the complexity of the design and the method of the mask application to the substrate. The technique used in this work makes use of photographic prints to transfer the desired image to the substrate material.

25

The antenna patterns were cut from Rubylith film on a high precision coordinatograph. The coordinatograph is capable of resolution to 0.001 inch. All the masks were cut ten times larger than the required size and created to form positive images. That is, the areas of Rubylith that were cut and removed represent the areas on the substrate where copper was required to remain after etching. Once all the Rubylith patterns were completed, the Rubylith film was placed on a large vertical illuminating screen. The Rubylith that was not cut from the film blocked all radiation emitted by the screen's lamp, while the light freely passed through the clear cut out areas. A simple reflex camera mounted on a track was then adjusted along the track to a predetermined position such that the image the camera produced was exactly ten times smaller that the Rubylith pattern. Once the camera was properly aligned, the shutter was opened to expose a photographically coated high resolution glass plate. This glass plate acted as the "film" in the camera and was developed in the standard solutions of developer, stopper, and fixer. Once the development of the glass plates was completed, the plates served as extremely accurate masks for the photo-etching process.

An alternative, and relatively new, technique uses a film, TEC-200, produced by the Meadowlake Corporation of

Northport, New York. This technique is much simpler than the photo mask technique, but is best used for simpler shapes since an exact scale drawing is required. An accurate CAD program used with a quality laser printer will produce the required artwork. Since there is no laser printer available for dedicated use in the manufacture of microstrip patch antennas, an alternative was developed. A computer program was written for use on the available equipment in the AFIT Anechoic Chamber. This program, MASK, and sample output can be found in appendix A. MASK is written in HP Basic and the Hewlitt Packard Graphics Language (HPGL) for use with an HP 9000 series computer and an HP 7470A Plotter. MASK is completely interactive and will produce a variety of high quality masks when a fine point drafting pen is used in the plotter. MASK is completely menu-driven and can produce positive or negative ground plane images, as well as a 15 degree mitered end for especially wide feed lines to avoid connector shorting. Once the high contrast drawings are produced, the TEC-200 film is loaded into a photocopier for image transfer onto the film. The film image is then placed on top of the substrate and a hot iron is used to transfer the image to the copper. Any small spots which do not transfer are covered using a simple resist pen. While this method is extremely simple, it did not produce completely satisfactory

results when used on the Duroid 5880.

Because of the time-consuming nature of the Rubylith film method, an alternative, simpler method was developed. A hybrid technique of the two methods described above was implemented. It was determined that the high contrast drawing produced using the MASK program can be accurately transferred to a clear sheet of thermal acetate using a ThermoFax machine. This image is then cut from the acetate and taped to a clear glass slide. This image taped to glass is then placed into a photographic reproducer and exposed to create an accurate mask. This process eliminates the extremely time consuming, expensive, and labor intensive Rubylith pattern production, as well as the requirement to photographically reduce the pattern to the required size.

Etching Process. Before the etching process was begun, it was imperative to ensure that the copper was completely clean and free of oxidation. Once the protective plastic covering was removed, the copper was scrubbed with acetone to remove any remaining adhesive material. The board was then immersed in dilute HCl for 15 to 30 seconds to remove oxidation. The board was then rinsed with acetone, methyl alcohol, and lastly deionized water. The board was then baked at 126 degrees Celsius for one hour to remove any moisture from the board. Moisture removal is critical to ensure that the photo resist will adhere to the copper.

Once the board was baked for one hour, it was allowed to cool to room temperature. The board was then placed on a photo resist spinner which uses a vacuum seal to secure the board to the spinning turntable. Approximately 1 milliliter of hexamethyl disiloxane, HMDS, a chemical agent that promotes the adherence of photo resist to copper, was placed in the center of the board. The board was then spun at 2000 rpm for 30 seconds, creating a thin uniform coating of HMDS across the copper surface. Next, approximately 1 milliliter of Microposit IIIS positive photo resist was applied to the center of the board and spun at 2000 rpm for 30 seconds. Positive photo resist creates a bond to the copper. This bond _s broken when exposed to high intensity UV light during the mask transfer process. Once the photo resist was applied, the substrate sample board was soft baked for 20 minutes at 75 degrees Celsius. The glass mask created photographically was inserted into the mask aligner. The board was then placed in the mask aligner. The mask aligner places the glass mask on top of and in contact with the copper-covered substrate. A high intensity UV light is activated above the glass mask during exposure. Thus, for positive photo resist, the UV light passes through the clear portions of the glass mask to break the photo resist's bond to the copper in these areas. The dark portions of the mask block the UV light from the photo resist and the photo

29

resist's bond to the copper remains intact in these areas.
For this application, it was determined by trial and error
that an exposure time of 2.5 minutes for this particular
photo resist spun on at this particular speed was best. The
exposed board was then placed on the photo resist spinner
for development. The board was spun at 500 rpm and sprayed
with a mixture of Microposit 303A developer and deionized
water (mixed at one part developer to four parts water) for
three minutes. The board was then rinsed for 30 seconds
with deionized water and air blown dry. Once dry, the board
was hard baked for 20 minutes at 135 degrees Celsius to
harden the photo resist. Once the hard baking was complete,
the antenna layers were ready for etching in Ferric
Chloride. The feed layer was much more difficult. The feed
layer required the same procedure to be applied to the
reverse side of the board. It was determined after many
unsuccessful attempts that it was best to first process the
feedline side of the board. This board was then hard baked
for an additional five minutes beyond the standard 20
minutes. Great care was necessary during application of the
HMDS, photo resist, and developer to the ground plane side
so that the already applied feedline mask was not scratched.
Once the masks were applied to both sides of the board, it
was necessary to touch up the ground plane side. Poor photo
resist adhesion spots were inevitable for two-sided

30

applications. This was overcome by repeated attempts to obtain a substrate board on which the poor spots occurred away from the aperture image. That is, the aperture image transferred perfectly, but spots occurred in the ground plane away from the aperture location. If ignored, the copper below these spots would be etched off when placed in the Ferric Chloride It was possible to correct these problem areas by directly applying the photo resist to any spots seen on the ground plane side using a cotton swab on large spots and a wooden toothpick on small spots. This extremely thick layer of photo resist was then hard baked at 135 degrees Celsius for 30 minutes. Once the hard baking was complete, the board was placed in a container of Ferric Chloride. Ferric Chloride was chosen as the etching agent since it is an active agent and is readily available in most 'lectronics stores. Active agents etch much more quickly than passive agents, so that under cutting along edges is minimized. The etching process took about 20 minutes for the feedline board and about 35 minutes for the patch antenna boards. The longer etch time for the single-sided boards was due to the requirement to etch away the entire copper layer from the back side of the patch antenna boards. It is possible to increase the etch rate by heating the Ferric Chloride, but it was found that this heat caused some of the photo resist to come loose and create unwanted holes

31

in the copper. Also, as a caution, the heated Ferric Chloride had to be vented since the heat drives off concentrated Chlorine gas from the solution. Once the unwanted copper was completely etched, the board was immediately removed from the Ferric Chloride and immersed in deionized water to neutralize any remaining Ferric Chloride on the board. The photo resist covering the protected copper areas was then removed using an acetone spray. The completed board was then cleaned with dilute HCl, acetone, and deionized water. Once the board was air blown dry, it was ready for assembly with the other layers.

Antenna Assembly. The first step in the assembly process required the holes for the alignment screws to be drilled with a drill press. Once the holes were finished, the final cut of each board was made using a razor blade. Cutting along the cell outline produced during the etching process left each substrate layer exactly the same size. The boards were cleaned once more in HCl and acetone. A coaxial connector was then soldered to the feedline and grounded to the aperture-containing ground plane. Special care was required in attaching the connector to avoid any gap between the connector and the mitered end of the feedline. Any air gap would introduce some unknown and unwanted input inductance. Each internal interface between layers was then coated with petroleum jelly and the

alignment screws were inserted and tightened. The petroleum jelly serves to fill the air gaps which occur due to the thickness of the copper when the layers are stacked. The petroleum jelly was recommended by Rogers Corporation for use with Duroid 5880 since the petroleum jelly has an effective permittivity near 2.2 . Once the alignment screws were tightened, the antenna was ready for measurement. It must be noted that even with alignment screws, some very small errors in alignment were unavoidable. This is in part due to the high conformability of the Duroid 5880 material. During the actual measurement process, a trial and error technique was used to position the layers for optimal operation. Once this position was determined, the screws were tightened and remained in place during all measurements.

IV.   Measurement Procedures and Results

This chapter contains a detailed description of the equipment used and the experimental set-ups for all measurements made in this study.   A simple verification of the manufacturer's quoted effective permittivity is described.   Plots of the voltage standing wave ratio (VSWR), return loss, Smith chart, and principal plane radiation patterns for the antennas are included.

Physical Characteristics Measurements

The Duroid 5880 substrate material is designed with a relative permittivity of 2.2 .   It is possible to make some simple measurements to come up with a good relative permittivity approximation for a sample of the material using the HP8510 to measure the appropriate S-parameters. Although this approximation could not be performed at these antennas' operating frequencies due to a lack of S and C band waveguides, the approximation was performed for 10 GHz. Figure 6 shows the configuration required to perform this measurement.   Once the HP8510 was properly calibrated, a sample piece of the Duroid 5880 with all the copper etched away was inserted in a mount and placed at the waveguides' junctions.   Measurements of S_{11} and S_{21} were taken, as well as the thickness of the sample under test. S_{11} is a
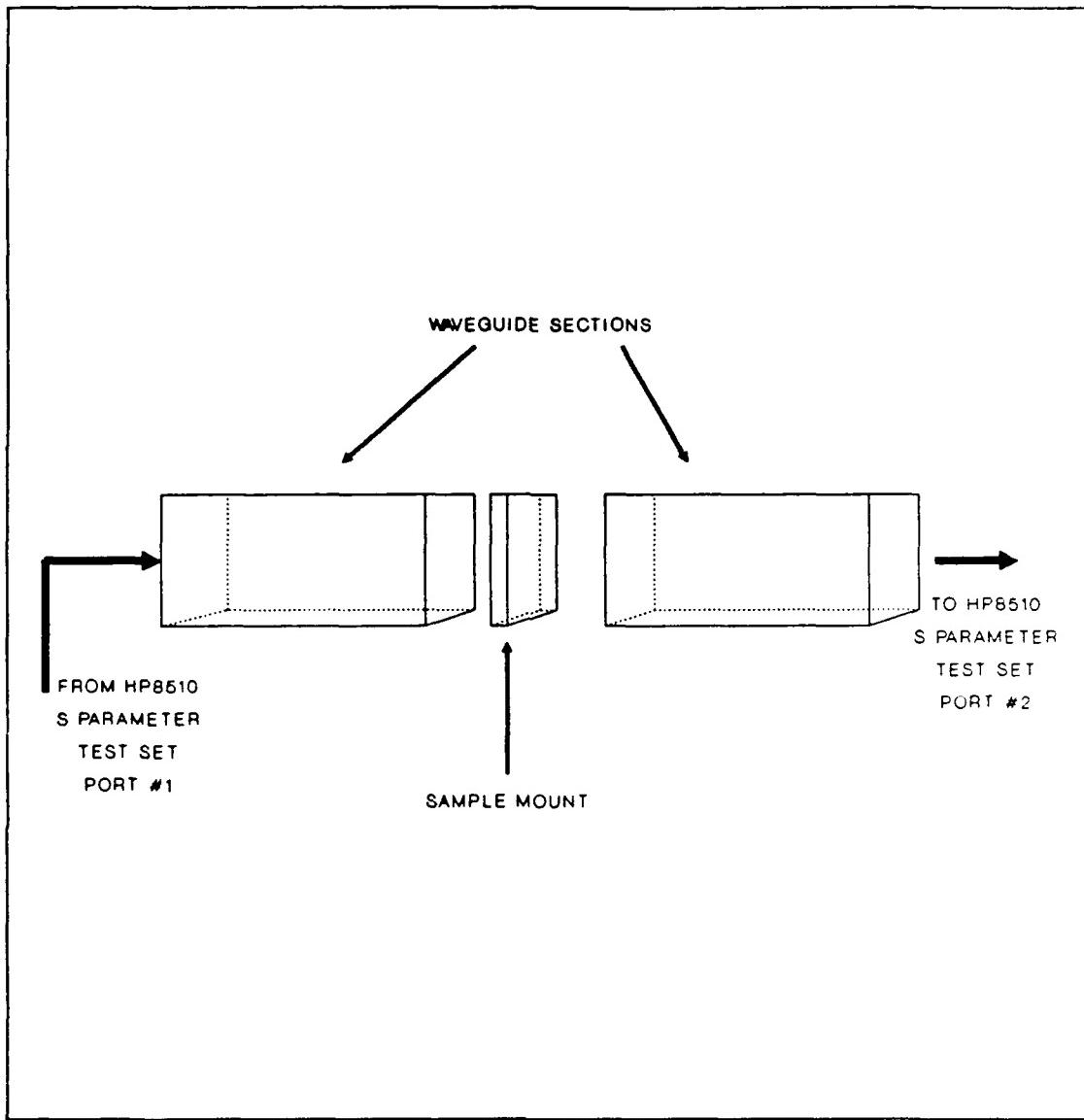
Figure 6.   Waveguide Set-Up for Permittivity Measurement

reflection coefficient seen at port 1, while S_{21} is a
transmission coefficient seen at port 2.   The measured
values were used in the following equations to make an
estimate of the relative permittivity of the sample (14:1).
The following equations define the reflection coefficient

(Γ) and a wave transmission factor (T) to account for the transmission of the wave through the sample (14:1-3).

$$\Gamma = \frac{Z_s - Z_o}{Z_s + Z_o} = \frac{\sqrt{\mu_r/\varepsilon_r} - 1}{\sqrt{\mu_r/\varepsilon_r} + 1}$$

$$T = \exp(-jd\omega\sqrt{\mu\varepsilon}) = \exp(-jd\frac{\omega}{c}\sqrt{\mu_r\varepsilon_r})$$

where

Z_s = impedance of sample

Z_o = free space characteristic impedance = 120π Ω

μ = permeability of sample

ε = permittivity of sample

μ_r = relative permeability of sample

ε_r = relative permittivity of sample

ω = radian frequency

d = sample thickness

From Eqs 6 and 7, S_{11} and S_{21} follow (14:1-3)

$$S_{11}(\omega) = \frac{(1 - T^2)\Gamma}{1 - T^2\Gamma^2}$$

$$S_{21}(\omega) = \frac{(1 - \Gamma^2)T}{1 - T^2\Gamma^2}$$

with

T = wave transmission factor from Eq (7)

Γ = reflection coefficient from Eq (6)

S_{11} and S_{21} are measured using the HP8510, while d is measured using a micrometer and the values are used below. Eqs 10 through 15 are algebraic manipulations leading to Eqs 16 and 17.

$$K = \frac{S_{11}^2(\omega) - S_{21}^2(\omega) + 1}{2S_{11}^2(\omega)} \qquad (10)$$

$$\Gamma = K \pm \sqrt{K^2 - 1} \qquad (11)$$

where

+ or - is chosen such that $|\Gamma| \le 1$

$$T = \frac{S_{11}(\omega) + S_{21}(\omega) - \Gamma}{1 - [\ S_{11}(\omega) + S_{21}(\omega)\ ]\Gamma} = |T|\ \angle\theta \qquad (12)$$

$$A = \ln(\frac{1}{T}) = \ln(\frac{1}{|T|}) + j(-\theta + 2\pi n) \qquad (13)$$

where

n = integer part of d/λ_g

37

$$\Lambda = \frac{1}{\sqrt{-[\frac{A}{2\pi d}]^2}} \qquad (14)$$

where

the root is chosen for $\text{Re}(\Lambda) \geq 0$

$$\lambda_c = 2a \qquad (15)$$

with

a = long dimension of the waveguide

Using the above algebraic steps leads to a value of μ_r and ε_r for a given test frequency (f_o) (14:1-3).

$$\mu_r = \frac{1 + \Gamma}{\Lambda(1 - \Gamma)\sqrt{\frac{1}{\lambda_o^2} - \frac{1}{\lambda_c^2}}} \qquad (16)$$

$$\varepsilon_r = \frac{(\frac{1}{\Lambda^2} + \frac{1}{\lambda_c^2})}{\mu_r}\lambda_o^2 \qquad (17)$$

For 10 GHz, ε_r was found to agree with the manufacturer's specification of 2.2 within 0.02.

Prior to assembly of the antenna, each of the layer's physical dimensions was measured to determine the amount of under cutting that occurred during the etching process. Under cutting is unavoidable and results in the final dimensions of the board being slightly less than the desired dimensions. Since this was the first microstrip antenna fabricated at AFIT, an accurate estimate for the percent of under cutting was unknown. Therefore, it was decided that the masks would be made at exactly the desired dimensions and the amount of under cutting would be determined after the etching process. It was realized that this dimensional error would cause the antenna's operation to be less than optimal, but since this work is to establish fabrication and measurement capabilities at AFIT, rather than fabricate an optimal antenna, this less than optimal antenna performance was acceptable. It must be recognized that under cutting is dependent on many factors such as area to be etched, etching characteristics, temperature of etching bath, etc. .

Table 1 lists the desired dimensions, the final dimensions, and the percent of under cutting witnessed for each of the layers. As can be seen, the percentage of under cutting is strongly dependent on the antenna component to be etched. It is interesting to note that the aperture suffered no under cutting. It was observed during the etching process that the Ferric Chloride would eat away the copper starting

TABLE 1

UNDER CUTTING OF ANTENNA DIMENSIONS

COMPONENT DIMENSION	DESIRED SIZE (mm)	ACTUAL SIZE (mm)	UNDER CUT (%)
FIRST PARASITIC PATCH WIDTH	25.0	24.7	1.20
FIRST PARASITIC PATCH LENGTH	25.0	24.7	1.20
ANTENNA PRIMARY PATCH WIDTH	25.0	24.8	0.80
ANTENNA PRIMARY PATCH LENGTH	25.0	24.8	0.80
SECOND PARASITIC PATCH WIDTH	26.5	25.5	3.77
SECOND PARASITIC PATCH LENGTH	26.5	25.8	2.64
FEEDLINE LENGTH	35.22	34.9	0.91
FEEDLINE WIDTH	5.0	4.9	0.20
APERTURE LENGTH	1.5	1.5	0.00
APERTURE WIDTH	11.0	11.0	0.00

from the exposed edges of the board and work in towards the patch or the feedline. Since the surface containing the aperture, the resist-protected ground plane, offered no exposed edge to the Ferric Chloride, the etchant had to attack the aperture evenly. This even etching action resulted in no discernable under cutting. Based on these

40

results, it can be seen that if the exact fabrication process described in this work is to be used, the masks should be made from zero to four percent larger than the desired sizes, depending on the antenna component. While this will not produce the desired size exactly, since under cutting is dependent upon so many variables, it should result in less error between the desired and the final dimensions of the antenna.

Antenna Radiation Characteristics Measurement

Once an antenna is designed and fabricated, it is still necessary to measure the radiation characteristics of the device. The measured characteristics validate the accuracy of theoretical predictions of performance, as well as revealing any fabrication errors.

Antenna Range. In order to make accurate measurements of the radiation characteristics of an antenna, it is necessary to suppress reflections and interference from the surrounding environment. In order to accomplish accurate antenna measurements, an indoor anechoic chamber dedicated to microstrip antenna measurements was constructed. The overall dimensions of the chamber were dictated by available working area and materials. A rectangular cross-sectioned chamber was selected to "simulate free-space and maximize the quiet zone" (3:708). The limiting cross-sectional size

41

factor was the height of the room available to house the anechoic chamber. Since this room's height was nine feet, the chamber's height and width were chosen to be eight feet to allow for clearance between the chamber and the room's roof. Based on financial and time restraints, only Radar Absorbing Material (RAM) that was already available could be used. At the time of construction, approximately 400 square feet of 18" pyramidal RAM, 48 square feet of 12" pyramidal RAM, and 72 square feet of flat RAM were available for use. Therefore, the wall lengths were set at 12 feet. In the frequency range of interest for this project, 12 feet satisfies the far-field requirement

$$r > \frac{2D_1D_2}{\lambda} \qquad (18)$$

with

> r = distance from the transmit antenna to the
>   receive antenna
>
> D_1 = diameter of the test antenna
>
> D_2 = diameter of the feed antenna
>
> λ = wavelength

Figure 7 shows the AFIT anechoic mini-chamber for antenna pattern measurements. Optimally the chamber should be longer to better simulate far field conditions at other
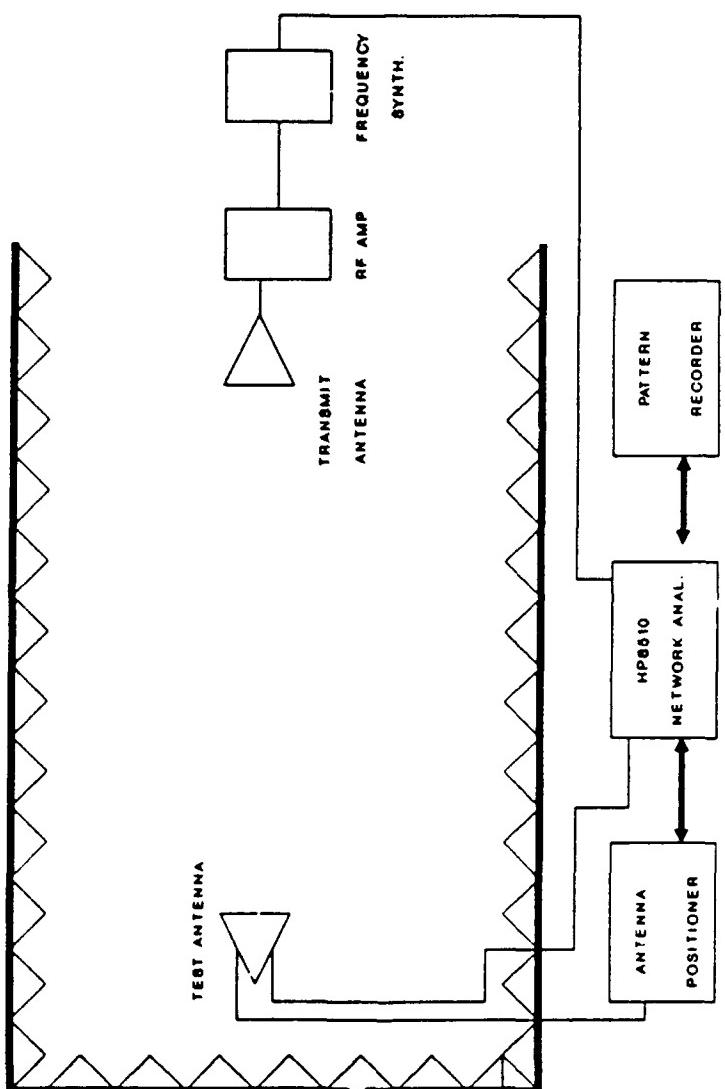
42

Figure 7. AFIT Anechoic Mini-Chamber

43

frequencies, so the chamber was constructed to facilitate extension of the length of the walls and ceiling as more RAM becomes available. This will allow the chamber to be used for larger antennas in the future. A skeletal frame of 2" by 2" lumber was first constructed for the two side walls and the back wall. Plywood was then attached to this frame and the RAM was cut and glued to the plywood. This method provided rigid, but manageable sections of the chamber. The back wall was attached directly to the existing room wall, thus acting as a stable foundation for the chamber. Large L-brackets were used to interconnect the side walls to the back wall. The roof was constructed by attaching two large beams to the top of each of the three sheets of 4' by 8' plywood used for the ceiling. The RAM was then glued to the bottom of the plywood. By working with only one sheet of RAM coated plywood at a time, it was possible to maneuver each of the three roof sections into place. Additionally, the beams provided excellent support and stabilization for the anechoic chamber. Once the walls and roof were in place, small pieces of RAM were used to seal any poorly joined seams. The floor was then covered by cutting and laying RAM on the cement without using glue. This allows access to the target pedestal by removing three pieces of RAM. The target pedestal consists of a simple wooden rectangular structure covered with flat RAM on the sides and

a collar of RAM on top to shield the receive antenna
rotator. Optimally, the chamber should be lined with
pyramidal absorber on the back wall to best absorb directly
incident energy, while the roof, ceiling, and walls should
use wedge-shaped absorber to funnel the incident energy to
the back wall for absorption, as opposed to reflecting the
energy into the quiet zone. The quiet zone for this
particular anechoic chamber can be estimated using the
following two equations, allowing a $\pi/8$ phase variation
across the wavefront and 1 dB downrange amplitude variation
(14:2-5).

$$D = \frac{R}{8.2} \qquad (19)$$

with

      D = quiet zone depth (in feet)

      R = distance between antennas (in feet)

$$L = \frac{2.218}{\sqrt{f}} \qquad (20)$$

with

      L = quiet zone width (in feet)

      f = operating frequency (in GHz)

Based on these equations and the anechoic chamber being used at 4.0 GHz with an antenna separation of 10 feet, the quiet zone is 1.11 feet wide by 1.22 feet deep.

Equipment Configuration. The equipment configuration used in the AFIT anechoic mini-chamber is shown in Figure 7. The heart of this system is the HP8510 Network Analyzer. The HP8510 is a vector network analyzer. That is, it measures the phase as well as the magnitude of the device under test. There are two basic types of measurements made by the HP8510: transmission measurements and reflection measurements. For antenna characteristic measurements, the reflection measurements (return loss, VSWR, and input impedance) are of interest. The HP8510 system has four main components: source, test set, receiver, and display processor. First, a source provides the RF signal. Second, a test set is used to separate the RF signal and send part to the device under test and the remainder to the processor as a reference signal for comparisons. Third, a receiver processes the signals. Last, the display processor unit receives the data from the receiver for use. The display processor can output to a CRT, a printer, a plotter, or a disk. The HP8510 computes all measurements by calculating the S-parameters for the device under test. Once these S-parameters are known, the HP8510 can make simple vector algebraic conversions to display such things as the VSWR,

46

reflection coefficient, impedance, etc. .

VSWR and Return Loss Measurement. For a one-port

device, such as a microstrip antenna, the VSWR and the

return loss are easily measured using an HP8510 Network

Analyzer in conjunction with an S-parameter test set. The

antenna is connected to port #1 while port #2 is connected

to an HP08515 termination collar. With the antenna

appropriately connected, the return loss is simply the S11

magnitude displayed in logarithmic form. Alternatively, the

VSWR can be determined from the simple relationship:

$$\text{VSWR} = \frac{1 + |\Gamma|}{1 - |\Gamma|} \qquad (21)$$

with

Γ = reflection coefficient

This simple calculation is performed internally by the

HP8510. The measurement is taken over a frequency range of

interest and plotted. Figure 8 shows the return loss for

the primary antenna (parasitic antenna patch of 2.47 cm by

2.47 cm). Figure 9 shows the VSWR for the same antenna.

The VSWR bandwidth is generally defined as that frequency

range over which the VSWR is less than 2:1, although values

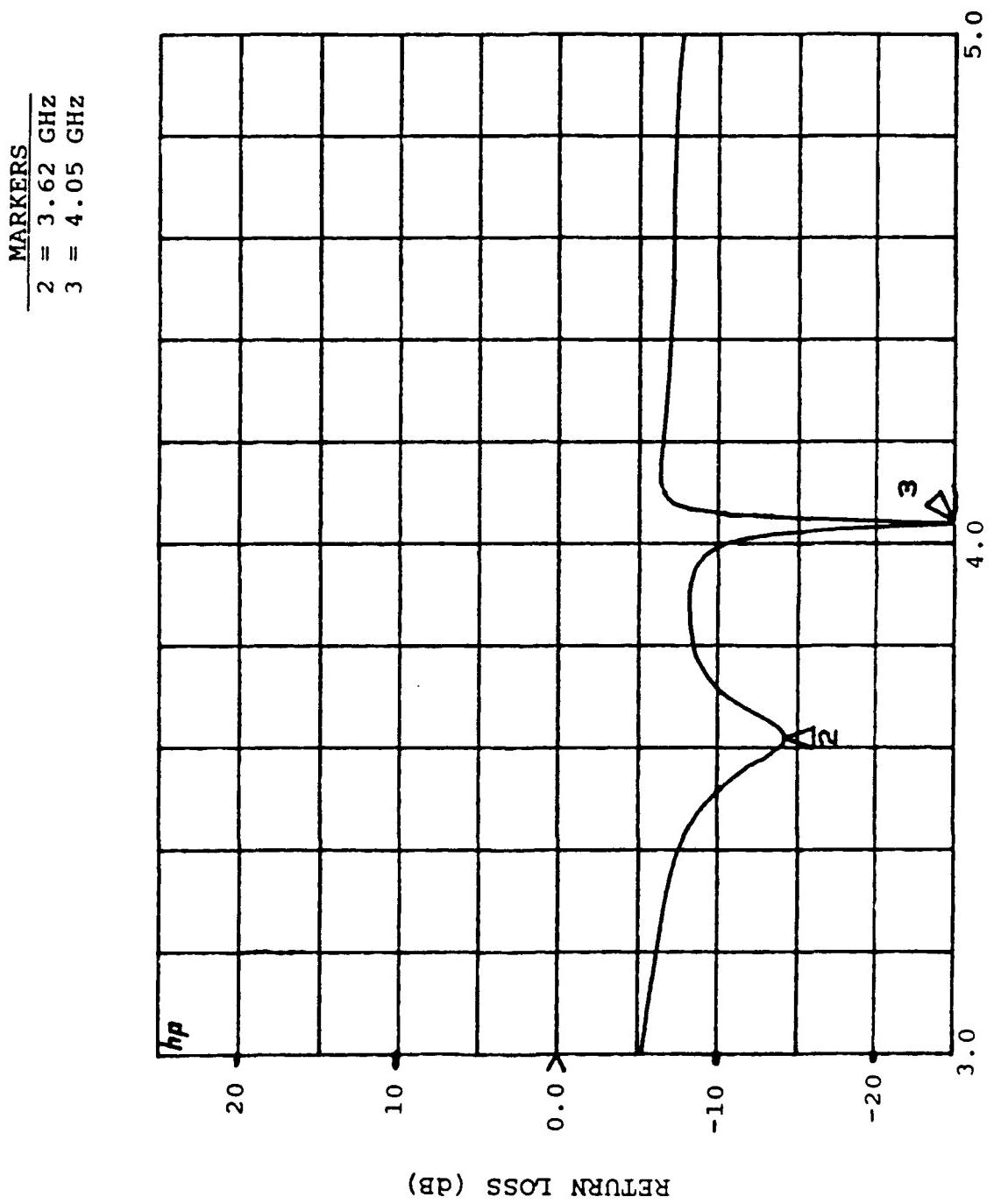of as high as 3:1 have been used in other studies. It can

47

MARKERS
2 = 3.62 GHz
3 = 4.05 GHz

FREQUENCY (GHz)

RETURN LOSS (dB)

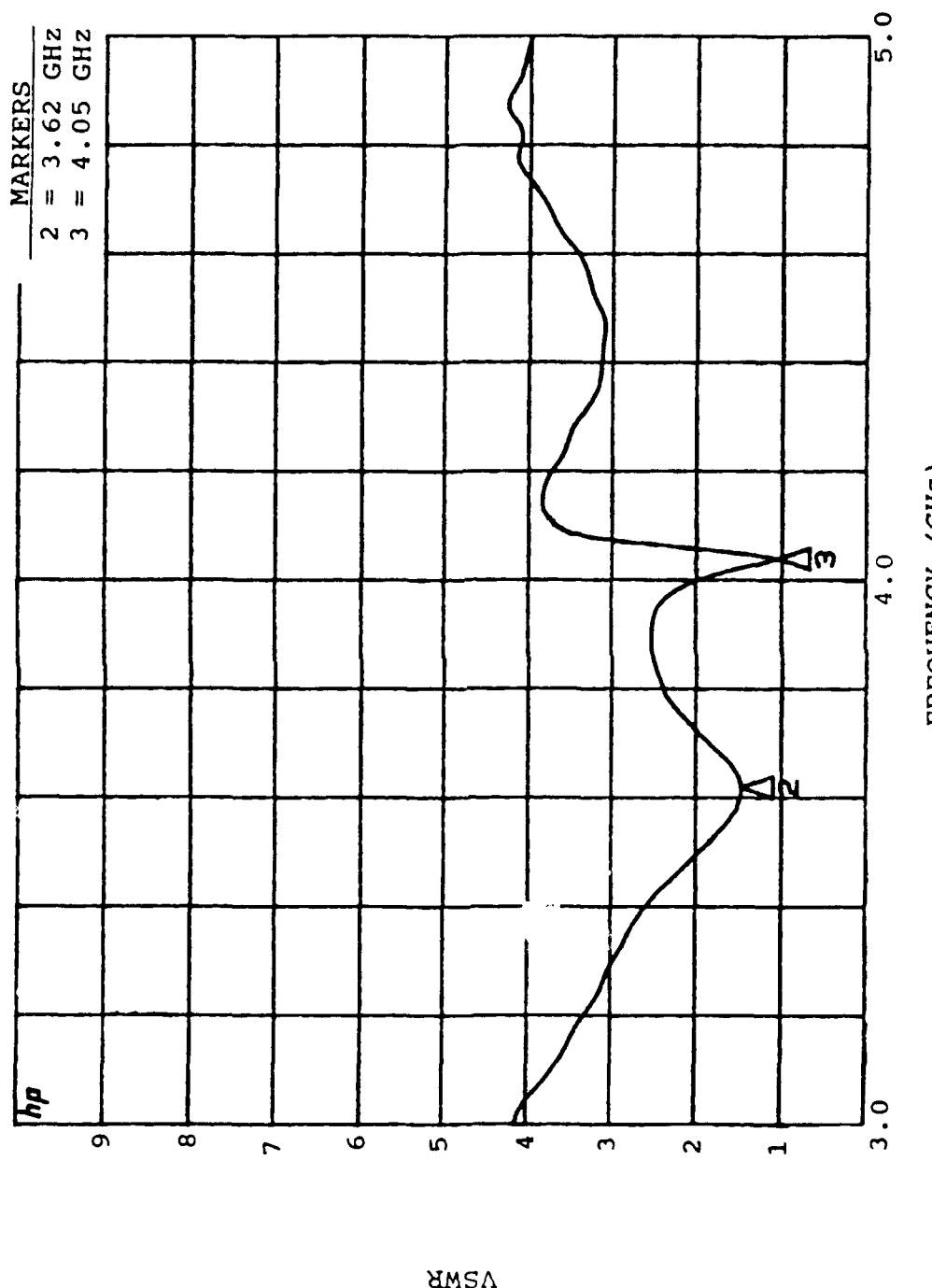Figure 8.   Primary Antenna Return Loss

Figure 9. Primary Antenna VSWR

49

be seen from Figure 9 that the primary antenna displays more

of a dual frequency characteristic, rather than the desired

single wide bandwidth since the VSWR is approximately 2.5

from 3.7 GHz to 3.95 GHz. This problem is most likely caused

by the under cutting during the etching process. That is,

the dimensional variation from the desired design causes

small shifts in the two resonant valleys. It is expected

that if no under cutting had occurred, that the two resonant

valleys would have merged at a VSWR value less than 2. It

is interesting to note that if the VSWR bandwidth

requirement of less than 2:1 is relaxed to a VSWR

requirement of less than 2.5:1, then the primary antenna

VSWR bandwidth can be calculated from Eq (22)

$$ BW = \frac{| \ f_2 - f_1 \ |}{f_c} * 100\% \qquad (22) $$

with

f_1 = first frequency for VSWR=2.5

f_2 = last frequency for VSWR=2.5

f_c = center frequency of band for VSWR<2.5

This gives the primary antenna a VSWR bandwidth of about

17.45% centered at 3.73 GHz for the relaxed VSWR requirement

of 2.5. It is recognized that relaxing the VSWR requirement

inflates the bandwidth, but it is obvious that stacking

50

patches is most effective for increasing the bandwidth over conventional microstrip patch antennas. Figures 10 and 11 show the return loss and the VSWR, respectively, for the secondary antenna (parasitic antenna patch of 2.58 cm length by 2.55 cm width). As can be seen from Figure 11, this antenna exhibits poorer VSWR bandwidth characteristics than the primary antenna with only the 3.45 GHz to 3.65 GHz band with a VSWR of less than two (VSWR bandwidth = 5.6%, centered at 3.55 GHz). Even with the relaxed VSWR requirement, the bandwidth is only 9.9% centered at 3.52 GHz. This must be attributed to the under cutting of the secondary antenna's parasitic patch of between 3-4%.

Input Impedance Measurement. Input impedance for an antenna can be measured using the HP8510 system by connecting the antenna to port #1 and again terminating port #2. This measurement is then performed over a swept frequency range and plotted on a Smith chart. Figures 12 and 13 are the Smith charts for the primary and secondary antennas, respectively. These plots illustrate the frequency dependence of the input impedance. Each plot typifies the inductive loop on the Smith chart generated by each patch. Since the antennas measured here contain two patches, two loops are discernable. It should also be noted that the inductive loops are centered on the Smith charts center since the feedline is designed at 50 ohms.

51
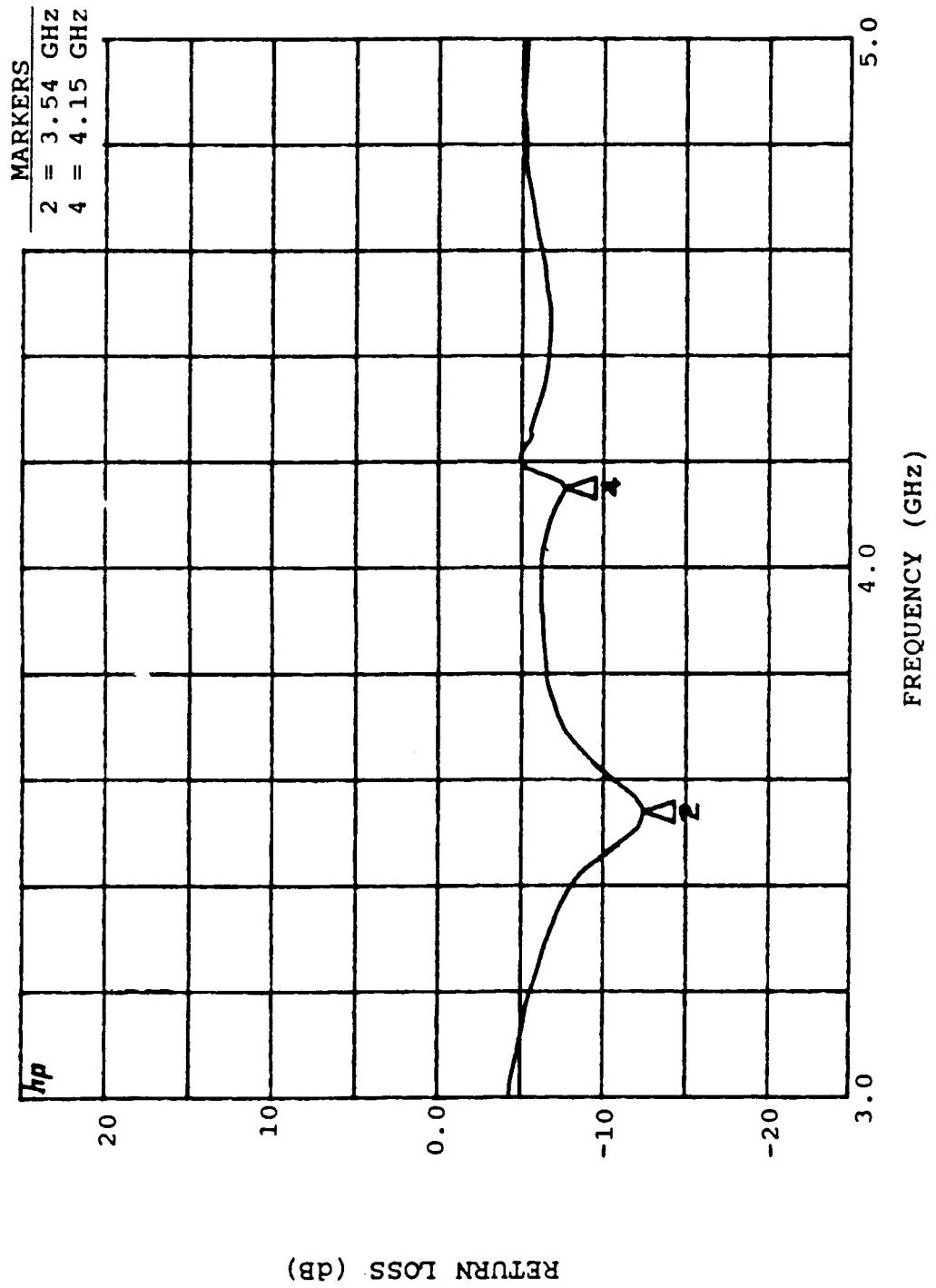
Figure 10. Secondary Antenna Return Loss

52
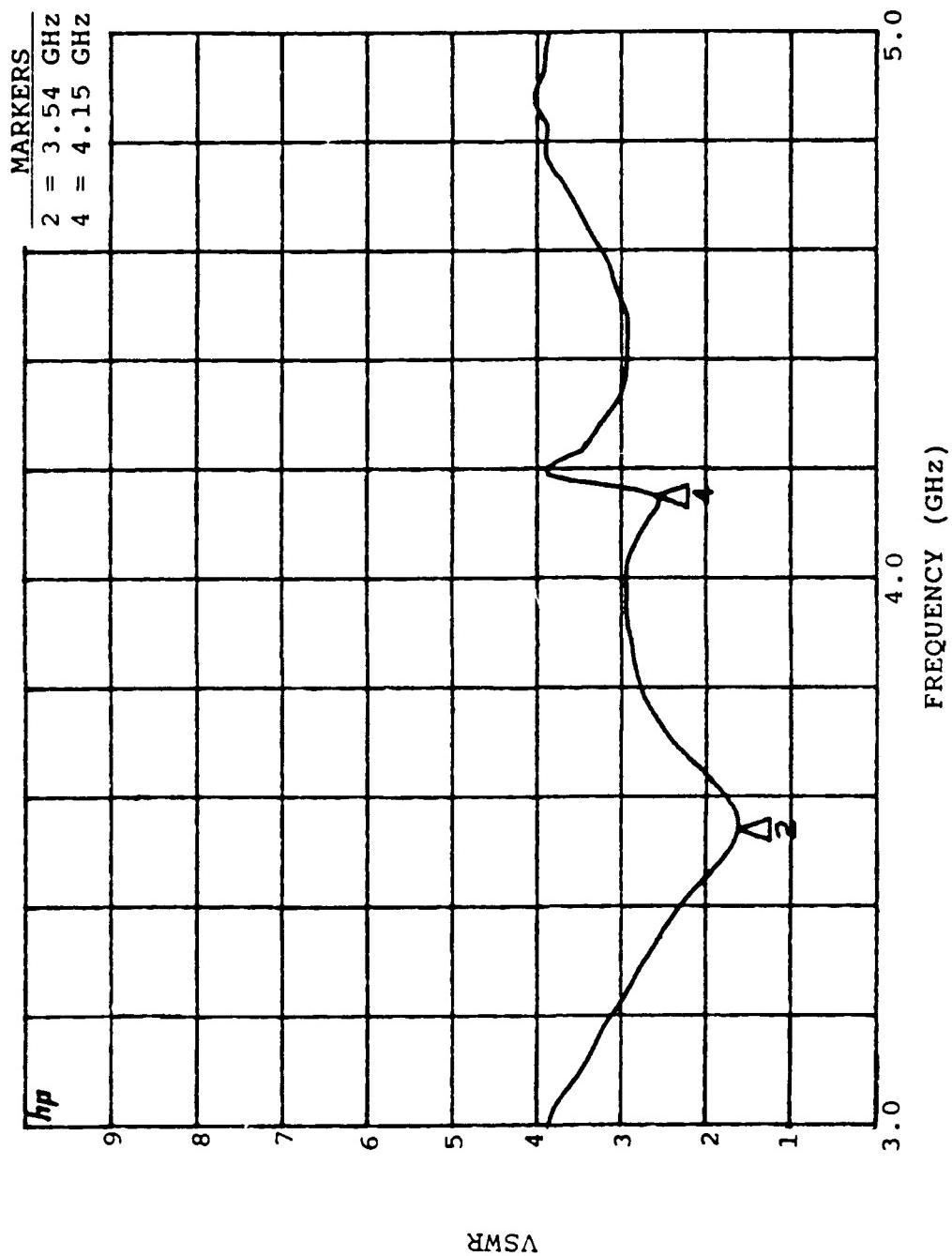
Figure 11. Secondary Antenna VSWR

53

S11
REF 1.0 Units
5 200.0 mUnits/
▽ 47.541 Ω -39.953 Ω
hp

MARKERS
1 = 3.6 GHz
2 = 3.7 GHz
3 = 3.8 GHz
4 = 3.9 GHz
5 = 4.0 GHz
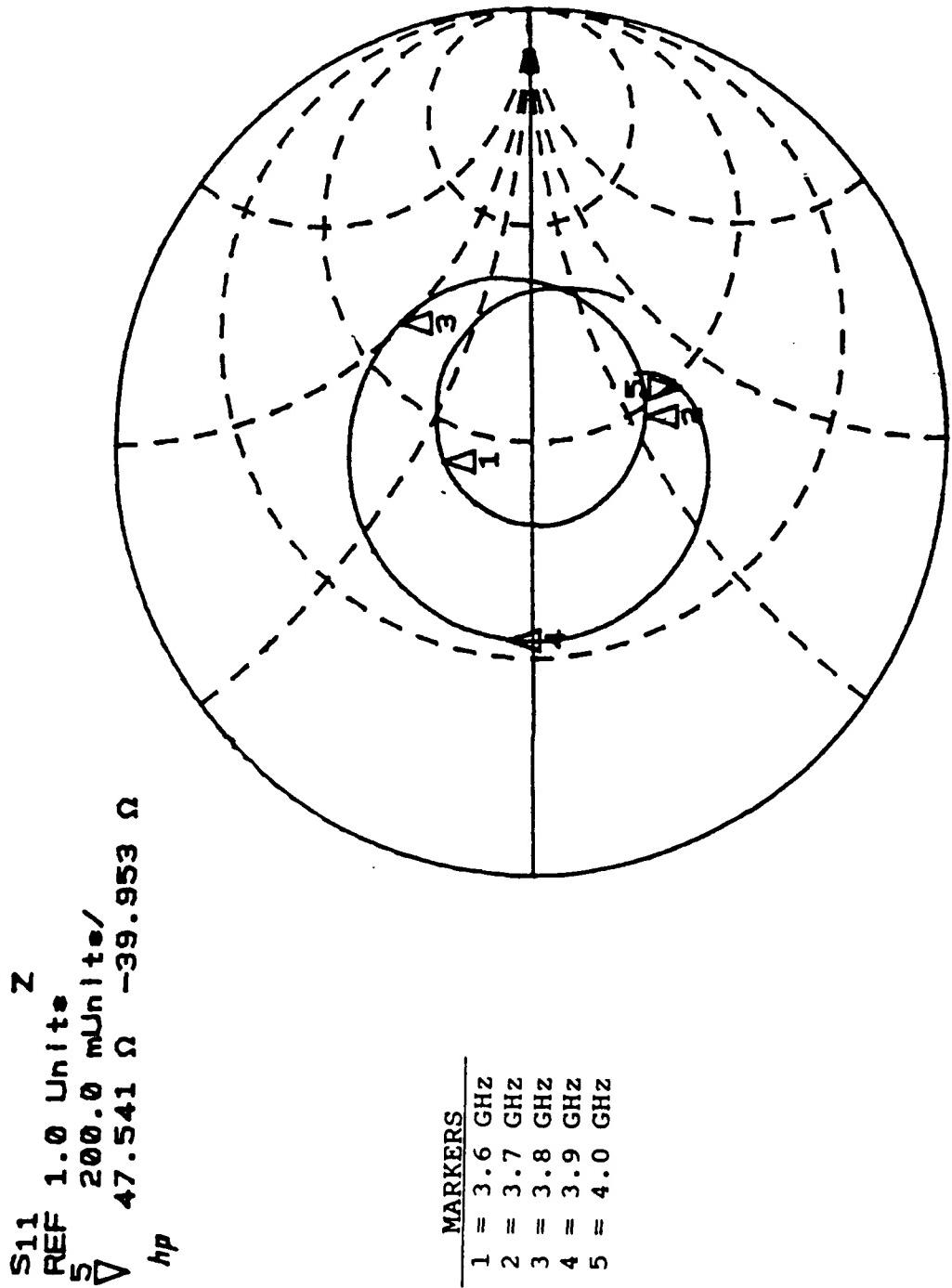
Figure 12. Primary Antenna Smith Chart

Figure 13. Secondary Antenna Smith Chart

S11
REF 1.0 Units
2 200.0 mUnits/
▽ 24.362 Ω -1.6172 Ω

hp

MARKERS
1 = 3.55 GHz
2 = 3.65 GHz
3 = 3.75 GHz
4 = 3.85 GHz
5 = 3.95 GHz

Antenna Pattern Measurements. Antenna patterns for
both the E-plane and the H-plane were taken for each of the
two antennas. In each measurement, the microstrip antenna
was used as the receive antenna in the chamber with a
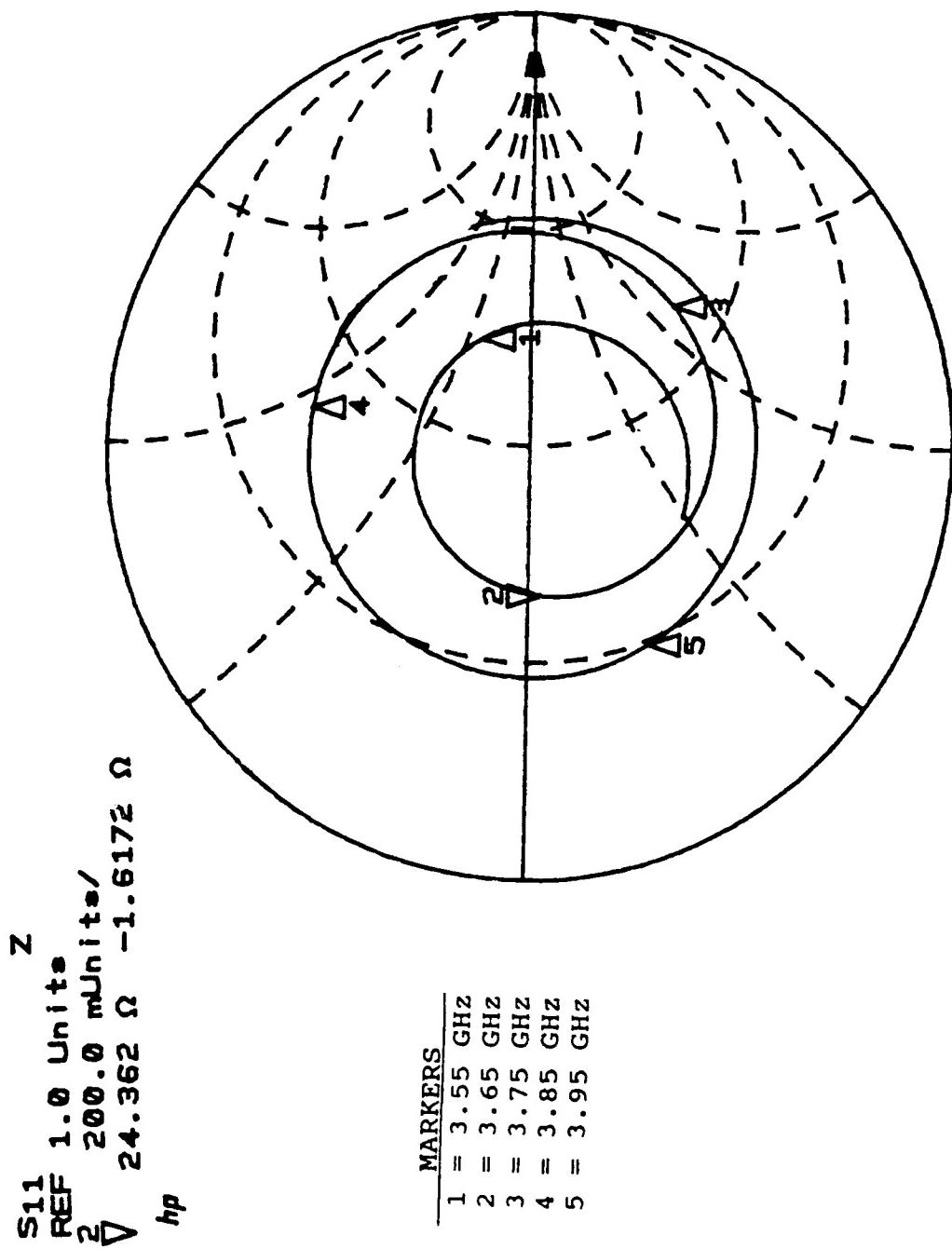standard gain broadband (2.0 - 18.0 GHz) horn antenna used
as the transmit antenna. The microstrip antenna was mounted
to an antenna positioner turntable. Optimally, the
microstrip antenna's output is fed into the HP8510 system
and plotted on a pattern recorder. Figure 7 shows a block
diagram of this pattern measurement configuration. In order
to use this configuration, the antenna positioner controller
must have an available interface allowing the positioner to
be slaved to the HP8510. During the time of this project,
only a positioner without an interface port was available,
so an alternative temporary measurement configuration was
employed to make the antenna pattern measurements. Figure
14 shows this configuration. Since pattern measurements are
made of the power received by the antenna at some aspect
angle relative to the peak power received, it was possible
to use a Boonton 4300 RF Digital Power meter to determine
the power output for the antenna. The standard gain horn
antenna (AEL H-1498), an HP8350B Sweep Oscillator, and an
HP8349B Microwave amplifier served as the transmit portion
of the configuration. The sweep oscillator was set to a
constant frequency of 3.7 GHz for the measurements. The

56
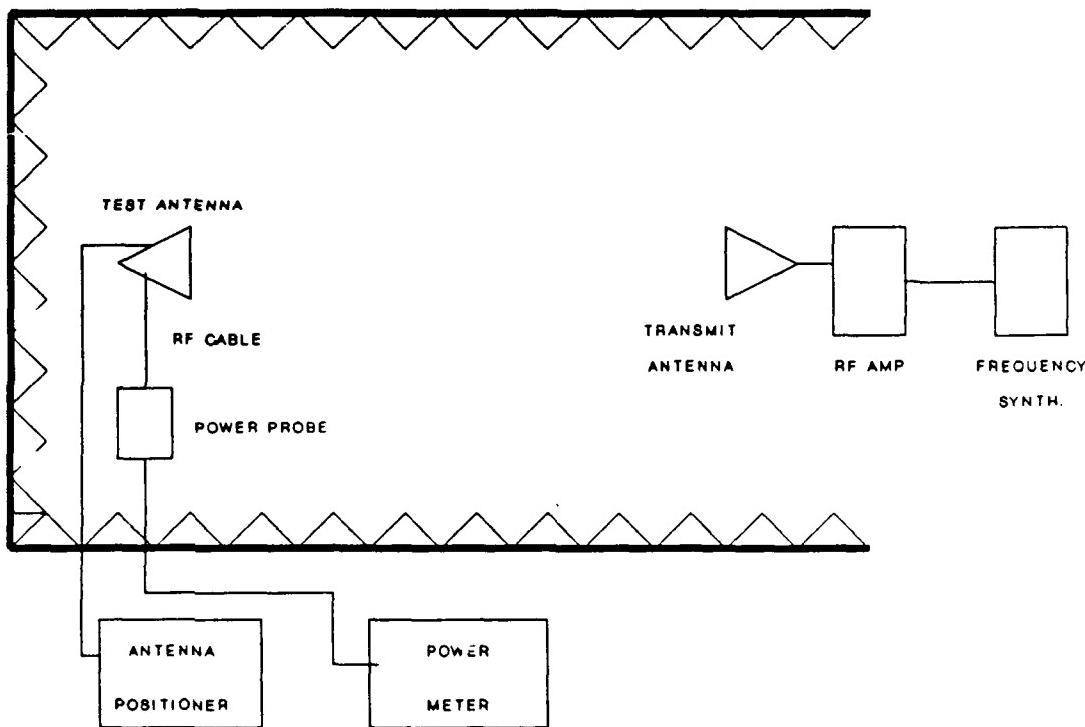
Figure 14. Pattern Measurement Configuration

microstrip antenna was mounted to the turntable and

connected via low loss cable to the power probe. The power

probe was then covered with RAM to minimize external

reflections from the probe. The microstrip antenna was then

slowly rotated until the peak power received was noted on

the power meter. This peak power served as the zero

reference for the particular pattern to be taken. Once the

power reference was set, the antenna was rotated one degree

at a time and the relative power reading recorded. Figures

15 and 16 show the E-plane and H-plane patterns for the primary antenna, respectively. Figures 17 and 18 show the E-plane and H-plane patterns for the secondary antenna, respectively. Each of the pattern plots depict the typical microstrip patch antenna radiation characteristics. The patterns' 3 dB beamwidths were on the order of 100 degrees in the E-plane and 80 degrees in the H-plane, as expected. In particular, the primary antenna's E-plane has a 3 dB beamwidth of 102 degrees and H-plane beamwidth of 83 degrees. The secondary antenna exhibited a 3 dB beamwidth 100 degrees, while the H-plane beamwidth was 87 degrees. The typical basic patch antenna pattern exhibits a cosine-type shape with varying degrees of backlobes. It should be noted that some asymmetry is evident in the E-plane patterns due to the connector location. Additionally, during measurement the power meter cable unavoidably interfered during part of the E-plane pattern measurements. The H-plane patterns do not suffer from this blockage or the connector asymmetry. Some ripple is evident, particularly in the H-plane patterns, and is attributed to surface wave effects induced on the ground plane containing the aperture. As mentioned in Chapter 2, it is desirable to have a ground plane on the order of four wavelengths. This was not physically possible due to limitations imposed during the photo masking operation and etching. Specifically, the mask

Figure 15. Primary Antenna E-Plane Pattern at 3.7 GHz

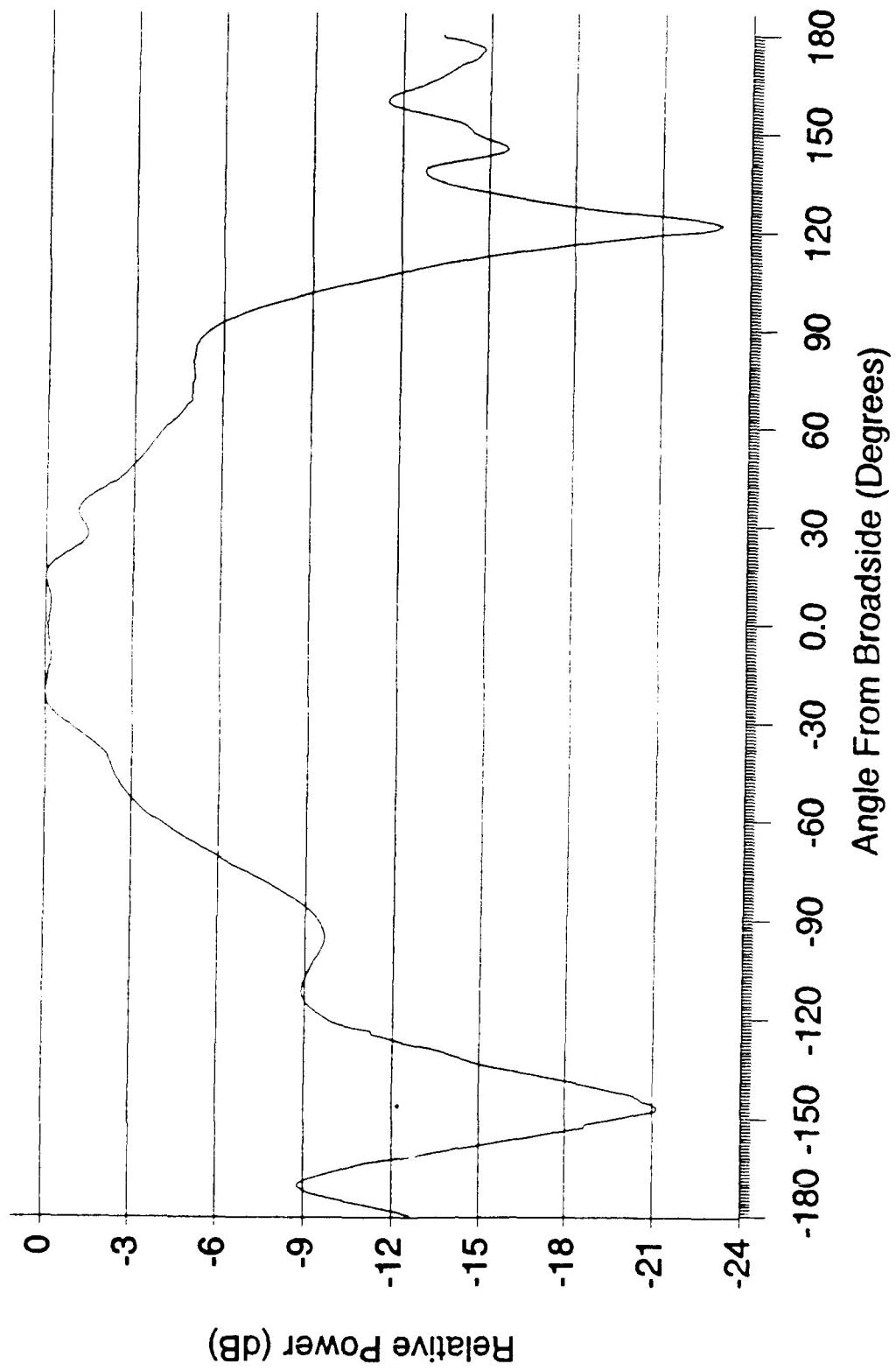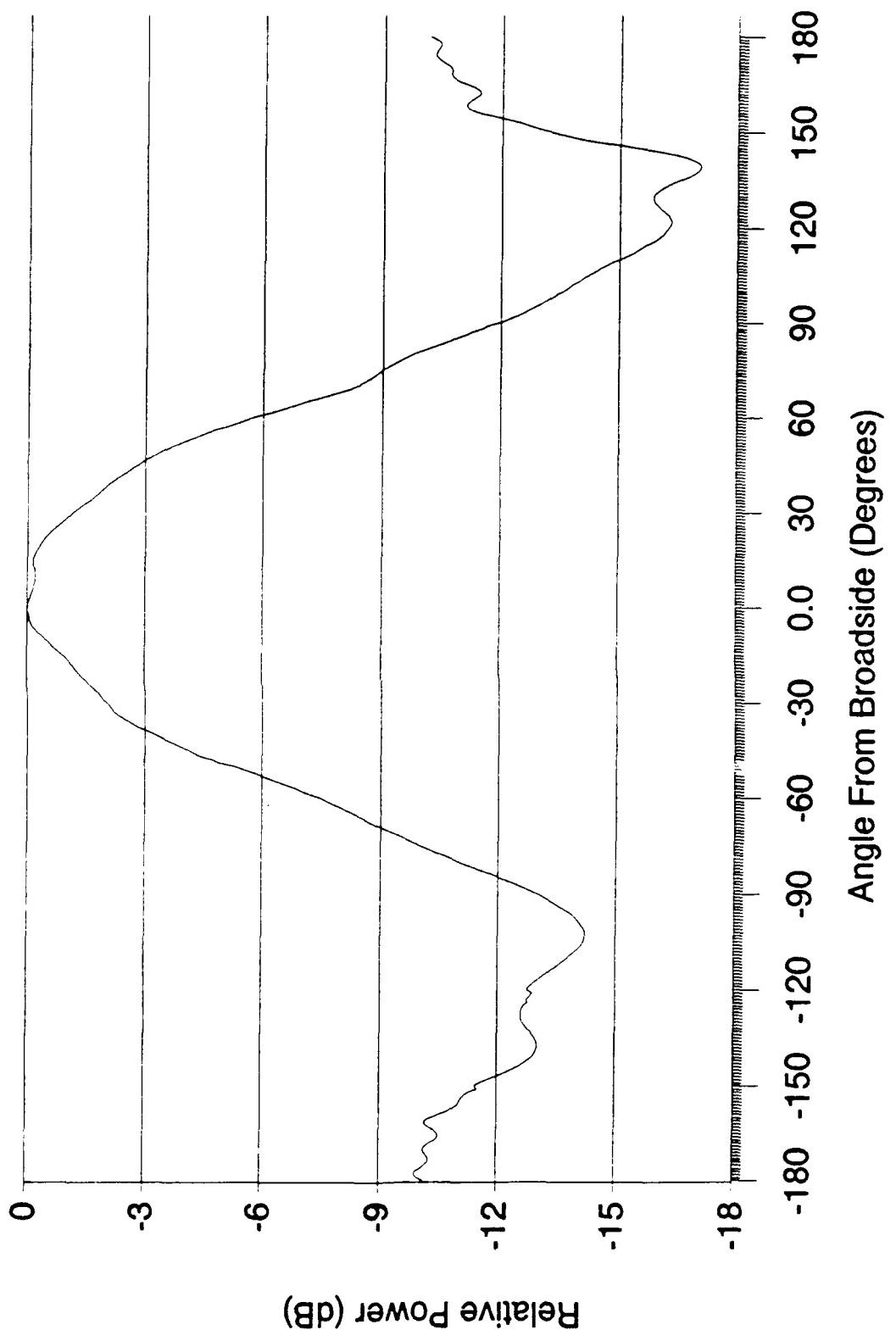Figure 16. Primary Antenna H-Plane Pattern at 3.7 GHz
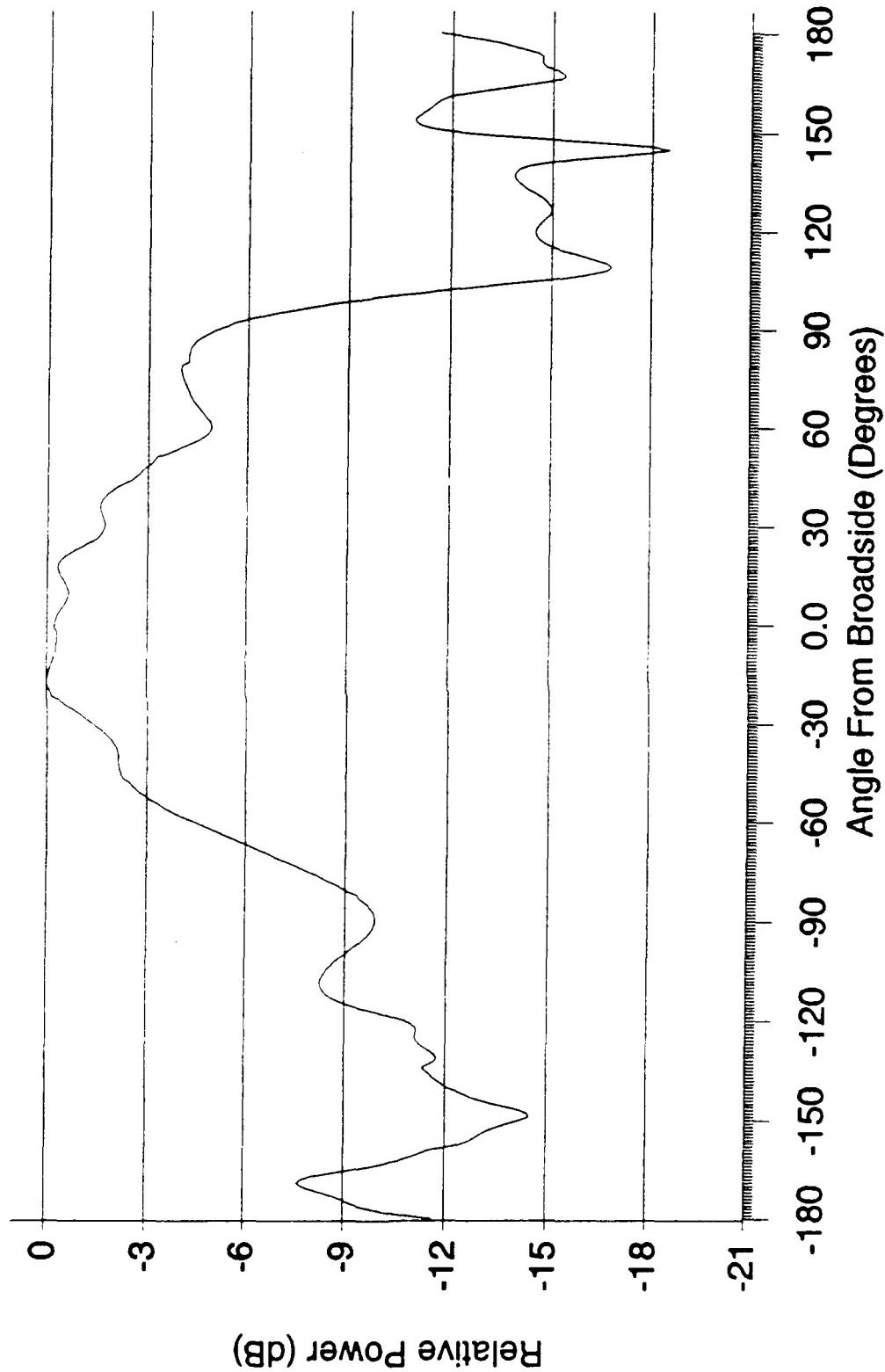
Figure 17. Secondary Antenna E-Plane Pattern at 3.7 GHz
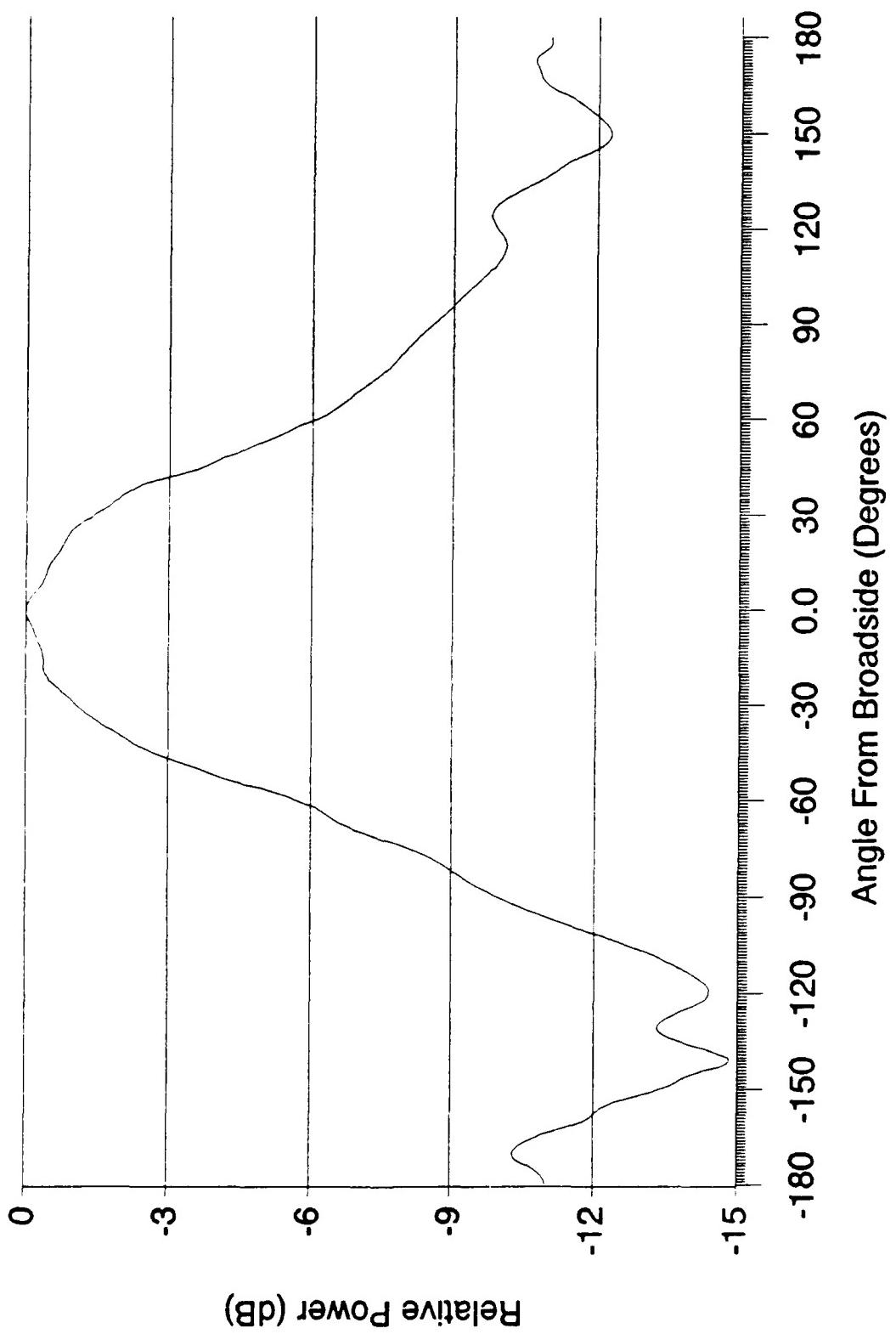
Figure 18.   Secondary Antenna H-Plane Pattern at 3.7 GHz

aligner can only accommodate a 2.12 inch by 2.12 inch substrate square. The back lobes evident in each of the patterns are typical, but are evidently corrupted by the presence of the uncovered microstrip feedline on the backside of the antenna.

V. Conclusion

The purpose of this study was to establish a
fabrication and measurement capability for aperture-fed
stacked patch microstrip antennas. The theory behind the
operation of basic microstrip patch antennas was discussed,
as well as the motivating factors behind the development of
the aperture-fed stacked patch microstrip antenna. The
broader bandwidth characteristic is the driving reason
behind the stacked patch configuration. The freedom of
substrate choice, increased available substrate area for
patch elements, and increased feedline isolation are
benefits of the aperture-feed design.

The selected antenna designs were described in detail,
as well as the reasons for their selection. The entire
fabrication process was discussed, from mask production
through final assembly. Measurement equipment, facility
descrip ions and methods of operation were provided, as well
as the actual measurements of the return loss, VSWR, input
impedance, and E and H-plane radiation pattern measurements
for the two antennas constructed during the course of this
study.

Conclusions

The efforts of this study were intended to provide AFIT with the capability to fabricate and measure aperture-fed stacked patch microstrip antennas.

Fabrication. It was determined that facilities at the Cooperative Electronics and Materials Laboratory designed for photo etching silicon wafers can be used to successfully photo etch microstrip antenna components. Through the use of the computer program, MASK, accurate artwork can easily be produced. This artwork can then be transferred to acetate and photographically transferred to glass slides for use in a photo mask aligner. It was determined that positive photo resist will successfully protect the copper from Ferric Chloride etchants. Although the process described in this study produces acceptable results, it does seem to suffer from severe under cutting for some antenna component designs. The percent under cutting by component was determined and tabulated. By suitably enlarging the artwork, much of the under cutting effects can be minimized. The importance of working with copper surfaces absolutely free of oxidation was made painfully clear during the many failed attempts to produce the antennas of this study.

Measurement. A small anechoic chamber dedicated to antenna pattern measurements was constructed. The two antennas built for this study did not perform optimally, but

performed acceptably. In particular, the antennas' two resonances did not quite merge completely to form the desired wide bandwidth (VSWR < 2). This is attributed to the adverse effects caused by the under cutting during etching. However, if the VSWR requirement is relaxed to 2.5, the primary antenna exhibited a bandwidth of nearly 18%. Both antennas displayed typical microstrip patch radiation patterns. The E-plane 3 dB beamwidths were approximately 100 degrees, while the H-plane 3 dB beamwidths were approximately 80 degrees. All the patterns were essentially cosine-shaped with varying degrees of backlobes. The backlobes suffered from distortion due to the uncovered microstrip feedline on the backside of the antenna. Some asymmetry was produced in the E-plane because of the location of the connector and blockage caused by the cable to the power probe. A small degree of rippling in the patterns, particularly the H-plane patterns, was due to the small size of the ground plane, which was limited by fabrication capabilities.

Recommendations for Further Study

Other avenues of study to improve the fabrication and measurement capability for aperture-fed stacked patch microstrip antennas, as well as further investigation of these antennas, include:

1. The fabrication technique described in this study produced acceptable results, but could be improved. In particular, only square and rectangular shapes were produced. Also, the positive photo resist used may very well be less than optimal. It is suggested that the fabrication process could be optimized through improvement of the MASK program to include many geometries, determination of the optimal photo resist solutions and techniques, and determination of an accurace model for under cutting of design components.

2. The small anechoic chamber produced for this study provides AFIT with a facility dedicated to the examination of the radiation characteristics of small antennas. This facility could be greatly improved through automation. A complete characterization of the anechoic chamber, to include the exact quiet zone, noise floor, etc. , could be performed while making upgrades and improvements to the chamber. As more RAM becomes available, the chamber should be extended in length to improve the far field nature of the chamber. Once an HP9800 series computer becomes available, the entire pattern measurement operation should be automated. The addition of an antenna positioner with an interface port will further facilitate automation of this chamber. Software should be written for use with the HP8510 and the antenna positioner.

3. Although the two antennas produced for this study did not perform optimally, they did make evident the improved bandwidth of the stacked patch design. Also, the VSWR characteristics of the two antennas varied greatly with just a change in the parasitic patch size between the two antennas. Many theoretical predictions are available in the literature for varying the parasitic patch size, but there is a decided lack of published experimental results to such studies. It is suggested that an investigation be conducted for a variety of aperture-fed stacked patch microstrip antennas varying only the parasitic patch size.

4. The primary role of the aperture-fed stacked patch microstrip antenna is as an element in an array. Although this thesis does not establish the capability to build and measure large arrays, certainly small arrays could be built for study. In particular, the mutual effects of the elements of the array upon each other should be studied, as well as the operating characteristics of the array.

Appendix: Artwork Creation Program

This appendix presents the computer program, MASK, written to create the artwork used to create the photo masks needed for the photo etching process. Figure 19 shows examples of the artwork produced by MASK when used with an HP7440A plotter with a .35 mm tipped drafting pen. It should be noted that standard felt tipped pen are unsatisfactory for high precision artwork since felt tipped pens tend to blur fine details. This program was written for the Hewlitt Packard 9800 series computers and the HP7440A Graphics Plotter. The program is written in HP Basic and HP Graphics Language (HPGL) and is completely interactive and menu driven. MASK is capable of producing high quality drawings of rectangular patch antennas, aperture containing ground planes, and microstrip feed lines. MASK includes the options to scale up all drawings as input with the magnification factor, is written to produce both positive and negative ground plane images, and includes an option to miter the feedline-connector junction to avoid shorting especially wide feedlines. The user also selects the plotter pen width factor to account for the use of pens with different width tips.
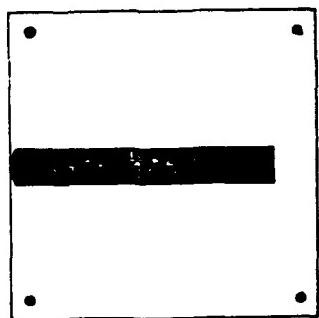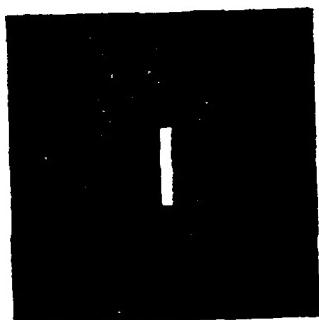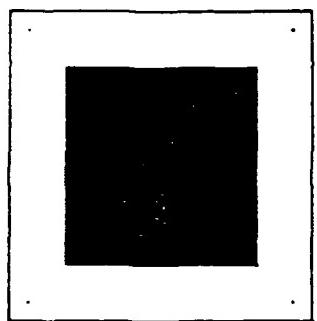
Figure 19.   Sample MASK Program Artwork

```
10      !PROGRAM: "MASK"
20      !THIS PROGRAM PRODUCES THE ARTWORK FOR APERTURE-FED
30      !STACKED PATCH MICROSTRIP ANTENNAS
40      !NOTE: THIS PROGRAM REQUIRES BINS "GRAPH" AND "GRAPHX"
50      REAL A,B,C,Cl,Cw,D,E,F,G,H,I,J,K,L,L1,L2,M,Pl,Pw,W1,W2
60      !P IS THE # OF PLOTTER UNITS (.025 mm/UNIT) USED
70      !BETWEEN SUCCESSIVE LINES TO FILL IN (DEPENDENT ON PEN
80      !TYPE USED)
90      OUTPUT KBD;"K";
100     PRINT "CHOOSE A VALUE BETWEEN 1 AND 10 FOR YOUR"
110     PRINT "PLOTTER PEN'S THICKNESS."
120     PRINT "1 = FINEST PEN CHOICE"
130     PRINT "10 = THICKEST PEN CHOICE"
140     INPUT "PEN CHOICE ?",P
150     IF P<1 OR P>10 THEN GOTO 90
160     PRINTER IS 1
170     GINIT
180     GRAPHICS ON
190     OUTPUT KBD;"K";
200     PRINT "SELECT AN OPTION"
210     PRINT "1 - RECTANGULAR PATCH ARTWORK"
220     PRINT "2 - RECTANGULAR APERTURE ARTWORK"
230     PRINT "3 - STRIPLINE ARTWORK"
240     PRINT "4 - EXIT PROGRAM"
250     INPUT "CHOICE ?",Z
260     IF Z=1 THEN GOTO 320
270     IF Z=2 THEN GOTO 840
280     IF Z=3 THEN GOTO 1240
290     IF Z=4 THEN GOTO 2020
300     GOTO 190
310     !RECTANGULAR PATCH ARTWORK OPERATIONS
320     INPUT "ENTER CELL LENGTH IN MILLIMETERS",Cl
330     INPUT "ENTER CELL WIDTH IN MILLIMETERS",Cw
340     INPUT "ENTER PATCH LENGTH IN MILLIMETERS",Pl
350     INPUT "ENTER PATCH WIDTH IN MILLIMETERS",Pw
360     INPUT "ENTER MAGNIFICATION FACTOR INTEGER",X
370     !I=40 PLOTTER UNITS/MILLIMETER
380     I=40*X
390     !COMPUTE CELL & PATCH EDGE POINTS IN PLOTTER UNITS
400     A=5125-(Cl/2*I)
410     B=5125+(Cl/2*I)
420     C=5125-(Pl/2*I)
430     D=5125+(Pl/2*I)
440     E=3879-(Cw/2*I)
450     F=3879+(Cw/2*I)
460     G=3879-(Pw/2*I)
470     H=3879+(Pw/2*I)
480     !COMPUTE POINTS FOR ALIGNMENT HOLES
```

```
490    J=A+100
500    K=B-100
510    L=E+100
520    M=F-100
530    !INITIALIZE PLOTTER AND TURN SCALE OFF
540    PRINTER IS 705
550    PRINT "IN;SC;"
560    PRINT "SP1"
570    !DRAW CELL OUTLINE
580    PRINT "PU";A;E
590    PRINT "PD";B;E;B;F;A;F;A;E
600    PRINT "PD";A-P;E-P;B+P;E-P;B+P;F+P;A-P;F+P
610    PRINT "PD";A-P;E-P
620    !DRAW AND FILL PATCH
630    PRINT "PU";C;G
640    FOR X=C TO D STEP 2*P
650       PRINT "PD";X;G;X;H
660       PRINT "PD";X+P;H;X+P;G
670    NEXT X
680    !DRAW ALIGNMENT HOLES
690    PRINT "PU";J;L
700    PRINT "PD"
710    PRINT "CI10"
720    PRINT "PU";J;M
730    PRINT "PD"
740    PRINT "CI10"
750    PRINT "PU";K;M
760    PRINT "PD"
770    PRINT "CI10"
780    PRINT "PU";K;L
790    PRINT "PD"
800    PRINT "CI10"
810    PRINT "PU"
820    PRINTER IS 1
830    GOTO 160
840    !APERTURE ARTWORK OPERATIONS
850    INPUT "ENTER APERTURE LENGTH IN MILLIMETERS",Al
860    INPUT "ENTER APERTURE WIDTH IN MILLIMETERS",Aw
870    INPUT "ENTER CELL LENGTH IN MILLIMETERS",Cl
880    INPUT "ENTER CELL WIDTH IN MILLIMETERS",Cw
890    INPUT "ENTER MAGNIFICATION FACTOR INTEGER",X
900    !I=40 PLOTTER UNITS/MILLIMETER
910    I=40*X
920    !COMPUTE APERTURE & CELL END POINTS IN PLOTTER UNITS
930    A=5125-(Cl/2*I)
940    B=5125+(Cl/2*I)
950    C=5125-(Al/2*I)
960    D=5125+(Al/2*I)
970    E=3879-(Cw/2*I)
980    F=3879+(Cw/2*I)
```

```
990    G=3879-(Aw/2*I)
1000   H=3879+(Aw/2*I)
1010   INPUT "SELECT IMAGE TYPE:  POSITIVE=1, NEGATIVE=2",Y
1020   !INITIALIZE PLOTTER, TURN SCALE OFF, AND SELECT A PEN
1030   PRINTER IS 705
1040   PRINT "IN;SC;SP1"
1050   IF Y=1 THEN GOTO 1080
1060   IF Y=2 THEN GOTO 490
1070   GOTO 1010
1080   FOR X=A TO B STEP 2*P
1090     IF X>C AND X<D THEN
1100        PRINT "PD";X;E;X;G
1110        PRINT "PU";X;H
1120        PRINT "PD";X;H;X;F
1130        PRINT "PD";X+P;F;X+P;H
1140        PRINT "PU";X+P;G
1150        PRINT "PD";X+P;G;X+P;E
1160     ELSE
1170        PRINT "PU";X;E
1180        PRINT "PD";X;E;X;F
1190     END IF
1200   NEXT X
1210   PRINT "PU"
1220   PRINTER IS 1
1230   GOTO 160
1240   !STRIPLINE ARTWORK
1250   OUTPUT KBD;"K";
1260   PRINT "CHOOSE STRIPLINE TYPE:"
1270   PRINT "1 - STANDARD STRIPLINE"
1280   PRINT "2 - 15 DEGREE MITERED EDGE STRIPLINE"
1290   INPUT "CHOICE ?",C1
1300   IF C1=1 THEN GOTO 1330
1310   IF C1=2 THEN GOTO 1500
1320   GOTO 1250
1330   INPUT "ENTER CELL LENGTH IN MILLIMETERS",Cl
1340   INPUT "ENTER CELL WIDTH IN MILLIMETERS",Cw
1350   INPUT "ENTER STRIPLINE LENGTH IN MILLIMETERS",Sl
1360   INPUT "ENTER STRIPLINE WIDTH IN MILLIMETERS",Sw
1370   INPUT "ENTER MAGNIFICATION FACTOR INTEGER",X
1380   !I=40 PLOTTER UNITS/MILLIMETER
1390   I=40*X
1400   !COMPUTE CELL & STRIPLINE EDGE POINTS IN PLOTTER UNITS
1410   A=5125-(Cl/2*I)
1420   B=5125+(Cl/2*I)
1430   C=A
1440   D=A+(Sl*I)
1450   E=3879-(Cw/2*I)
1460   F=3879+(Cw/2*I)
1470   G=3879-(Sw/2*I)
1480   H=3879+(Sw/2*I)
```

```
1490   GOTO 490
1500   INPUT "ENTER CELL LENGTH IN MILLIMETERS",Cl
1510   INPUT "ENTER CELL WIDTH IN MILLIMETERS",Cw
1520   INPUT "ENTER STRIPLINE LENGTH IN MILLIMETERS",Sl
1530   INPUT "ENTER STRIPLINE WIDTH IN MILLIMETERS",Sw
1540   INPUT "ENTER MAGNIFICATION FACTOR INTEGER",X
1550   !I=40 PLOTTER UNITS/MILLIMETER
1560   I=40*X
1570   !CALCULATE CELL & STRIPLINE EDGE POINTS
1580   A=5125-(Cl/2*I)
1590   B=5125+(Cl/2*I)
1600   C=A
1610   D=A+(Sl*I)
1620   E=3879-(Cw/2*I)
1630   F=3879+(Cw/2*I)
1640   G=3879-(Sw/2*I)
1650   H=3879+(Sw/2*I)
1660   !COMPUTE POINTS FOR ALIGNMENT HOLES
1670   J=A+100
1680   K=B-100
1690   L=E+100
1700   M=F-100
1710   !INITIALIZE PLOTTER AND TURN SCALE OFF
1720   PRINTER IS 705
1730   PRINT "IN;SC;"
1740   PRINT "SP1"
1750   !DRAW CELL OUTLINE
1760   PRINT "PU";A;E
1770   PRINT "PD";B;E;B;F;A;F;A;E
1780   PRINT "PD";A-P;E-P;B+P;E-P;B+P;F+P;A-P;F+P
1790   PRINT "PD";A-P;E-P
1800   !DRAW ALIGNMENT HOLES
1810   PRINT "PU";J;L
1820   PRINT "PD"
1830   PRINT "CI10"
1840   PRINT "PU";J;M
1850   PRINT "PD"
1860   PRINT "CI10"
1870   PRINT "PU";K;M
1880   PRINT "PD"
1890   PRINT "CI10"
1900   PRINT "PU";K;L
1910   PRINT "PD"
1920   PRINT "CI10"
1930   PRINT "PU"
1940   !DRAW AND FILL STRIPLINE
1950   PRINT "PU";A+.26795*(3879-(H-G)/2);G
1960   FOR X=G TO H STEP 2*P
1970   PRINT "PD";A+.26795*ABS(X-3879);X;D;X
1980   PRINT "PU"
```

```
1990   NEXT X
2000   PRINTER IS 1
2010   GOTO 160
2020   OUTPUT KBD;"K";
2030   PRINT "ARTWORK SESSION ENDED"
2040   END
```

Bibliography

1. Bahl, I.J. and P. Bhartia. "Design Considerations in Microstrip Antenna Fabrication," _European Microwave Proceedings, 10_: 122-126 (1981).

2. -----. _Microstrip Antennas_. Dedham MA: Artech House, 1980.

3. Balanis, Constantine A. _Antenna Theory: Analysis and Design_. New York: Harper and Row, 1982.

4. Bhattacharjee, A.K. and others. "An Approach to the Computation of Input Impedance of Centre-Fed Rectangular Microstrip Antennas," _IEEE International Symposium Digest on Antennas and Propagation, 3_: 1169-1173 (1988).

5. Buck, A.C. and D.M. Pozar. "Aperture-Coupled Microstrip Antenna With a Perpendicular Feed," _Electronic Letters, 22_: 125-126 (30 January 1986).

6. Chang, Esin and others. "An Experimental Investigation of Electrically Thick Rectangular Microstrip Antennas," _IEEE Transactions on Antennas and Propagation, AP-34_: 767-772 (June 1986).

7. Chen, C.H. and others. "Broadband Two-Layer Microstrip Antenna," _IEEE International Symposium Digest on Antennas and Propagation, 1_: 251-254 (1984).

8. Das, Nirod K. _A Study of Multilayered Printed Antenna Structures_. PhD dissertation. University of Massachusetts, Amherst MA, 1989.

9. Garidol, F. E. "Design and Layout of Microstrip Structures," _IEE Proceedings, Part H, 135_: 145-157 (June 1988).

10. Hammerstadt, E. O. "Equations for Microstrip Circuit Design," _Proceedings of the European Microwave Conference, Hamburg, Germany_: 268-272 (September 1975).

11. Himdi, M. and others. "Analysis of Aperture-Coupled Microstrip Antenna Using Cavity Method," _Electronic Letters, 25_: 391-392 (16 March 1989).

12. Institute of Electrical and Electronics Engineers, Inc.
    IEEE Standard Test Procedures for Antennas. New York:
    IEEE Press, 1979.

13. James, J.R. and others. Microstrip Antenna Theory and
    Design. New York: Peter Peregrinus Ltd., 1981.

14. Joseph, Captain Philip J. Class handout distributed in
    ENG 626, Microwave Measurements I. School of
    Engineering, Air Force Institute of Technology (AU),
    Wright-Patterson AFB, OH, October 1989.

15. Lee, R.Q. and K.F. Lee. "Effects of Parasitic Patch
    Sizes on Multi-Layer Electromagnetically Coupled Patch
    Antenna," IEEE International Symposium Digest on
    Antennas and Propagation, 2: 624-627 (1989).

16. Lee, R.Q. and others. "Characteristics of a Two-Layered
    Electro-Magnetically Coupled Rectangular Patch
    Antenna," Electronic Letters, 23: 1070-1072 (24
    September 1987).

17. Mautz, Joseph, R. Electromagnetic Coupling Through
    Apertures. Contract F30602-79-C-0011. Griffiss Air
    Force Base NY: Rome Air Development Center, January
    1982 (AD-A112630).

18. Mullinix, Captain Daniel A., Laboratory Engineer.
    Personal interviews. Air Force Institute of
    Technology (AU), Wright-Patterson AFB, OH, 1 June
    through 15 September 1990.

19. Mullinix, Daniel A. and Daniel T. McGrath. "Rectangular
    Microstrip Patch Antenna Arrays." In-House Report RADC-
    TR-86-151. Rome Air Development Center, Hanscom Air
    Force Base MA, October 1986.

20. Pous, R. and D.M. Pozar. "Frequency-Selective Surface
    Using Aperture-Coupled Microstrip Patches," Electronic
    Letters, 25: 1136-1137 (17 August 1989).

21. Pozar, D.M. "Microstrip Antenna Aperture-Coupled to a
    Microstripline," Electronic Letters, 21: 49-50 (17
    January 1985).

22. Sabban, Albert. "A New Broadband Stacked Two-Layer
    Microstrip Antenna," IEEE International Symposium
    Digest on Antennas and Propagation, 1: 63-65 (1983).

23. Schaubert, Daniel H. and David M. Pozar. "Aperture Coupled Patch Antennas and Arrays," Proceedings of the Antenna Applications Symposium, 1: 135-154 (1986).

24. Tsao, C.H. and others. "Aperture-Coupled Patch Antennas with Wide Bandwidth and Dual Polarization Capabilities," IEEE International Symposium Digest on Antennas and Propagation, 3: 936-939 (1988).

VITA

Capt Christopher I. Terry ▮▮▮▮▮▮▮▮▮▮▮▮▮▮ ▮▮▮▮▮ in Key West, Florida. He graduated from high school in Jacksonville, Florida, in 1976. He enlisted in the Air Force in 1979 and served in California, Texas, Italy, and Maryland as a Russian Linguist. In 1983, he entered the University of Florida as part of the Air Force's Airman Education and Commissioning Program. Following receipt of a Bachelor of Science Degree in Electrical Engineering in May 1986, Capt Terry graduated from Officer Training School in August 1986. He then served as a research and development engineer for the ▮ ▮0th Electronic Security Wing at Fort Meade, Maryland, until entering the School of Engineering, Air Force Institute of Technology, in June 1989.

REPORT DOCUMENTATION PAGE

Public reporting burden for this collection of information is estimated to average 1 hour per response, including the time for reviewing instructions, searching existing data sources, gathering and maintaining the data needed, and completing and reviewing the collection of information. Send comments regarding this burden estimate or any other aspect of this collection of information, including suggestions for reducing this burden, to Washington Headquarters Services, Directorate for Information Operations and Reports, 1215 Jefferson Davis Highway, Suite 1204, Arlington, VA 22202-4302, and to the Office of Management and Budget, Paperwork Reduction Project (0704-0188), Washington, DC 20503.

1. AGENCY USE ONLY (Leave blank)	2. REPORT DATE December 1990	3. REPORT TYPE AND DATES COVERED Master's Thesis

4. TITLE AND SUBTITLE ESTABLISHMENT OF A FABRICATION AND MEASUREMENT CAPABILITY FOR APERTURE-FED STACKED PATCH MICROSTRIP ANTENNAS AT THE AIR FORCE INSTITUTE OF TECHNOLOGY

5. FUNDING NUMBERS

6. AUTHOR(S)

Christopher I. Terry, Captain, USAF

7. PERFORMING ORGANIZATION NAME(S) AND ADDRESS(ES)

Air Force Institute of Technology
WPAFB, OH 45433-6583

8. PERFORMING ORGANIZATION REPORT NUMBER

AFIT/GE/ENG/90D-61

9. SPONSORING / MONITORING AGENCY NAME(S) AND ADDRESS(ES)

10. SPONSORING / MONITORING AGENCY REPORT NUMBER

11. SUPPLEMENTARY NOTES

12a. DISTRIBUTION / AVAILABILITY STATEMENT

Approved for public release; distribution unlimited

12b. DISTRIBUTION CODE

13. ABSTRACT (Maximum 200 words)

Much time and effort has been applied to accurately model aperture-fed stacked patch microstrip antennas at the Air Force Institute of Technology (AFIT). The results of this study provide AFIT with the capability to fabricate and measure these antennas for comparison of measured radiation characteristics to the predicted characteristics. Basic microstrip patch antenna theory is reviewed, as well as the motivation leading to the development of aperture-fed stacked patch microstrip antennas. The fabrication process used to produce the two antennas manufactured for this study is described in detail. The construction of a small anechoic chamber for pattern measurements is discussed, and measurements of the return loss, VSWR, input impedance, and principal plane radiation patterns for the two antennas of this study are provided. Although the two fabricated antennas did not operate optimally due to under cutting during the etching process, the measurement results show the broader bandwidth characteristic of the stacked patch design. The results of this study are most useful as a guide to researchers starting an active microstrip patch antenna investigation.

14. SUBJECT TERMS Microstrip Patch Antenna, Antenna Fabrication, Antenna Pattern Measurement, Aperture-Feed

15. NUMBER OF PAGES 88

16. PRICE CODE

17. SECURITY CLASSIFICATION OF REPORT Unclassified	18. SECURITY CLASSIFICATION OF THIS PAGE Unclassified	19. SECURITY CLASSIFICATION OF ABSTRACT Unclassified	20. LIMITATION OF ABSTRACT UL

NSN 7540-01-280-5500